Archives of Microbiology (2025) 207:280
https://doi.org/10.1007/s00203-025-04480-3

ORIGINAL PAPER

Physiological and genomic insights into *Bacillus* sp. BRTN from Baratang mud volcano with emphasis on SUF system proteins

Karuna Soren[1] · Dibyendu Khan[1] · Ashutosh Kabiraj[1] · Urmi Halder[2] · Moitri Let[1] · Annapurna Chitikineni[3,4] · Rajeev K. Varshney[3,4] · Aparna Banerjee[5] · Rajib Bandopadhyay[1]

Received: 17 June 2025 / Revised: 9 August 2025 / Accepted: 9 September 2025 / Published online: 25 September 2025

Abstract

Bacterial genome analysis provides valuable insights into the identification of potential biomolecules for diverse biotechnological and therapeutic applications. Particularly, bacteria isolated from extreme environments such as mud volcanoes possess unique physiological and genetic traits that may offer novel opportunities for both in vitro studies and in silico drug target discovery. In this study, a total of 10 bacteria were isolated from Baratang mud volcano, located in Andaman and Nicobar Islands of India; of which strain BRTN was selected for further study based on its best ferrous sulfate ($FeSO_4$ MTC value 600 mg L^{-1}) tolerance capability and antibiotic sensitivity profile (resistant to Gentamycin, Streptomycin, Ceftriaxone, and Sulphatriad). Optimum growth of BRTN was found at pH 8.0 and it could tolerate up to 16% NaCl. The whole genome sequencing, assembly, and annotation identified that BRTN had the most proximity with *Bacillus* genera. The bacterium was associated with 3.35 Mb genome with 35.9% of GC content and harbored 3514 genes. Genome analysis revealed that Sulfur Utilization Factor (SUF) proteins was present in the accessory genome. Genome analyses confirmed the presence of *SufB*, *SufC*, *SufD*, *SufE2*, etc. SUF genes (non-homologous to human genome) that could be considered as potent targets to develop antimicrobial compounds. Furthermore, in silico analysis including homology modeling and receptor-ligand docking were carried out to characterize the selected SUF proteins and to assess their potentiality for functional inhibition by candidate ligands. Among all interactions, SufD showed best Vina score (−14.0) when it interacted with ChEMBL3921511, suggesting SufD protein as a potential drug target. Thus, the SUF system genes identified in this study may serve as promising targets for the development of novel antibacterial therapies.

Keywords Antibiotherapy · Extremophiles · Drug target · Fe–S cluster · Fe–S cluster biogenesis machinery · SUF system

Communicated by Kristina Beblo-Vranesevic.

✉ Rajib Bandopadhyay
rajibindia@gmail.com

1 Department of Botany, The University of Burdwan, Golapbag, Bardhaman, West Bengal 713104, India

2 Department of Pathology, Microbiology and Immunology, University of South Carolina School of Medicine, Columbia, USA

3 Center of Excellence in Genomics and Systems Biology, International Crops Research Institute for the Semi-Arid Tropics (ICRISAT), Hyderabad 502324, India

4 State Agricultural Biotechnology Centre, Centre for Crop and Food Innovation, Murdoch University, Murdoch 6500, Australia

5 Functional Polysaccharides Research Group, Instituto de Ciencias Aplicadas, Facultad de Ingeniería, Universidad Autónoma de Chile, Sede Talca, Talca, Chile

Introduction

Mud volcanoes harbor unique geological features in respect to wide range of temperature (30–120 °C) that may provide a window into subsurface biosphere; as it carries deep seated sediments, fluids, minerals, gases such as methane (CH_4), carbon dioxide (CO_2), hydrocarbon components along with many unexplored biological constituents of the Earth's sub-surface layer (Dimitrov 2002). Also, these volcanic eruptions are enriched of several metals such as Fe, Ni, Cd, Mn, Zn, Pb and As (metalloid) etc., posing high risks to the environment (Plumlee et al. 2008; Sholehhudin et al. 2019). Many extremophilic bacteria were reported from mud volcanoes including CH_4 tolerant, sulfur metabolizing, hydrocarbon degrading, multi-metal resistant, halophiles, thermophiles; viz. *Methylobacterium rhodesianum*,

Sulfurimonas crateris, *Pseudomonas stutzeri*, *Sideroxydans lithotrophicus*, *Mariprofundus ferrooxydans*, *Halomonas daqingensis* and *Thermoactinomyces vulgaris* etc. (Omoregie et al. 2008; Fru et al. 2012; Yang et al. 2012; Chen et al. 2015; Kokoschka et al. 2015; Tu et al. 2017; Ratnikova et al. 2020; Slobodkina et al. 2020). From the Baratang mud volcano (situated at Andaman and Nicobar Islands, India) different plant growth promoting, heavy metal resistant, organic matter degrading, thermostable enzyme producing, and bacteria with antioxidative properties like *Bacillus megaterium*, *Rhodococcus* sp., *Streptosporangium* sp., *Geobacillus toebii* etc. have been reported previously (Dhaker et al. 2011; Ilayaraja et al. 2014; Manna et al. 2021; Meena et al. 2023). Accordingly, it is evident that, mud volcano offers diverse research opportunities to harness associated microbiota for application in biodiversity exploration, environmental remediation, metal degradation, agriculture, plant growth promotion, industrial application, energy production, antibiotherapy, and more. On the other hand, modern approaches such as omics technologies, bioinformatics, and integrated genomic-proteomic database have revolutionized bacterial profiling, enabling the identification of new drug targets and accelerating drug discovery. (Fokunang and Fokunang 2022). Consequently, the everchanging environmental conditions of mud volcanoes act as powerful selective pressure to develop novel and extraordinary attributes in their resident microorganisms. While, in the present scenario, antibiotic-resistant bacteria (ARB) have emerged as a global health crisis due to poor governance, misuse and limited drug target innovation (Muzawazi et al. 2024). Parallelly, in this situation, pathogens are evolving novel resistance mechanisms, such as moderation of virulence factors, stress-response systems, efflux transporters and chaperones, beyond classical pathways *viz* mitigation of DNA inhibition, membrane disruption, or efflux system modification. Notably, many bactericidal antibiotics exert their effect by inducing oxidative stress, suggesting a shared mechanism underlying their lethality. However, rising multidrug resistance has prompted the search for alternative strategies. In view of this fact, scientists advised the co-selection theory of heavy metal and antibiotic resistance arises from shared resistant genes, regardless of which stressor is present (Halder et al. 2022). Therefore, in this present study, we explored whether metal and drug resistance mechanisms are related to bacterial oxidative stress mitigation via the SUF system. The SUF system assembles Fe–S clusters, which are vital for bacterial stress survival by acting as redox-sensitive switches that modulate transcription and translation under oxidative stress. These clusters also play essential roles in core functions such as respiration, photosynthesis, nitrogen fixation and gene regulation (Davies 1990; Dowling et al. 2017; Blahut et al. 2020; Elchennawi and Ollagnier de Choudens 2022; Baran et al. 2023). Mainly three types of Fe–S cluster biogenesis machinery are known till date from all domains of life, among which nitrogen fixations (NIF) system contributes to Fe–S cluster assembly and is essential to nitrogen fixing organisms. The Iron Sulfur Cluster (ISC) system encodes predominantly Fe–S cluster under normal condition. Whereas, expression of SUF system is upregulated under Fe limited condition and oxidative stress (Garcia et al. 2022). The principal mechanisms underlying Fe–S cluster biosynthesis and functionality are largely conserved across different organisms. These include mobilization of sulfur and iron, the formation of nascent Fe–S clusters on scaffold proteins, and the subsequent delivery of cluster to target protein (Nambi et al. 2015). Among diverse Fe–S cluster found across three domains of life, 2Fe-2S and 4Fe-4S types are most common, typically composed of Fe^{2+}/Fe^{3+} ions and sulfide (S^{2-}) (Pala et al. 2019; Gao 2020). Fe–S cluster assembly involves multiple proteins: SufBCD forms the scaffold for cluster formation, SufSE mobilizes sulfur from L-cysteine, SufA transfers the cluster to apoproteins, and SufU may substitute SufE in certain systems (Pérard and Ollagnier de Choudens 2018; Fontecave and Ollagnier-de-Choudens 2008). In host, as a part of the defense mechanism, oxidative stress is reported to be generated upon pathogenesis. However, a group of scientists suggested that pathogenic microorganisms such as *Mycobacterium tuberculosis*, *Escherichia coli* and *Plasmodium vivax* may overcome this stress with the help of SUF system (Pala et al. 2019; Lo Sciuto et al. 2024; Gorityala et al. 2024). Therefore, targeting Fe–S cluster biogenesis via SUF system inhibition offers a pathogen-specific strategy without compromising host integrity and presents a promising avenue to combat antibiotic resistance.

In this study, iron tolerant bacteria (ITB) were isolated from the Baratang mud volcano and characterized using maximum tolerable concentration (MTC) determination for $FeSO_4$, antibiotic susceptibility assays, polyphasic and phylogenetic profiling. Additionally, comprehensive genome analysis and in silico characterization were performed to investigate the correlation between experimental evidence of bacterial survival under oxidative stress and to hypothesized the role the SUF system in redox stress mitigation. Furthermore, a preliminary screening of SUF protein inhibitors was conducted to validate as a target candidate for anti-biotherapy.

Materials and methods

Sample collection, physicochemical characterization, and bacterial isolation

Mud sample was aseptically collected from Baratang mud volcano of Andaman and Nicobar Islands, India (13° 04′ 12.00″ N and 92° 28′ 12.00″ E). Inductively Coupled Plasma Atomic Emission Spectrophotometer (ICP-AES; Perkin Elmer, USA; Optical 2100DV) was used to quantify metals in the mud sample. Additionally, C, H, N, S concentration and C/N ratio of the mud sample were studied using Elemental analyzer (Vario EL III, Germany). Fourier Transform Infrared Spectroscopy (FTIR, Perkin Elmer, USA) analysis was used to detect the presence of functional groups in the sample.

Isolation of bacterial sample from mud

After the collection of mud sample from Baratang mud volcano sediment, 1.0 g sample was dissolved in 10 mL 0.9% NaCl solution (pre autoclaved), after 60 min incubation the solution was serially diluted (up to 10^{-4} dilution) and 100 µL sample solution was spread on starch casein agar media (SCA, HiMedia, India) ; containing casein-0.3 g L^{-1}, soluble starch-10 g L^{-1}, NaCl-2.0 g L^{-1}, KNO_3-2.0 g L^{-1}, K_2HPO_4-2.0 g L^{-1}, $CaCO_3$-0.02 g L^{-1}, $MgSO_4 \cdot 7H_2O$-0.05 g L^{-1}, $FeSO_4 \cdot 7H_2O$-0.01 g L^{-1}, agar-20 g L^{-1}, and pH-7.0 (Meena et al. 2023), and minimal salt agar (MSM) media with slight modification in media composition (K_2HPO_4-0.02 g L^{-1}, KH_2PO_4-0.02 g L^{-1}, $MgSO_4 \cdot 7H_2O$-0.03 g L^{-1}, $CaCl_2$-0.05 g L^{-1}, $NaNO_3$-0.5 g L^{-1}, NH_4Cl-0.5 g L^{-1}, glucose 5.0 g L^{-1}). After 72 h of incubation separate colonies was selected on the basis of their morphology and purified by quadrant striking method to get pure colonies on SCA.

Maximum tolerable concentration (MTC) of $FeSO_4$

All the bacterial isolates were grown in Luria Bertani (LB) broth, pH 7.0 (HiMedia, India) and an aliquot of the log phase culture($OD_{600\ nm} \sim 0.5$) were used as inoculum. Then, MTC of ferrous sulfate, $FeSO_4$ (HiMedia, India) of the selected isolates were determined by growing them ($OD_{600\ nm} \sim 0.5$) in minimal salt medium (MSM) with slight modifications containing K_2HPO_4-0.2 g L^{-1}, KH_2PO_4-0.2 g L^{-1}, $CaCl_2$-0.05 g L^{-1}, $MgSO_4$-0.03 g L^{-1}, $NaNO_3$-3.0 g L^{-1}, NH_4Cl-3.0 g L^{-1}, with yeast extract-0.1 g L^{-1}; pH-7.0. The cultures were then incubated at 37 °C for 48 h in 120 rpm supplemented with various concentrations of $FeSO_4$ (100, 200, 300, 400, 500, 600, 800, 1000 in mg L^{-1}) and absorbance were taken by using a visible spectrophotometer (Model LI-721, Lasany, India) at 600 nm wavelength.

Antibiotic sensitivity test

Disc diffusion assay was performed (Bauer et al. 1966) for antibiotic sensitivity test. After spreading of bacterial inoculums (100 µL) on Mueller Hilton Agar (MHA, HiMedia, India), pH 7.0 (Halder et al. 2020) different commercially available antibiotic discs (HiMedia, India) like amoxyclav (AMC-30 mcg), ampicillin (AMP-10 mcg), ceftazidime (CAZ-30 mcg), ceftriaxone (CTR-30 mcg), gentamicin (GEN-30 mcg), ofloxacin (OF-5 mcg), chloramphenicol (C-30 mcg), streptomycin (S-10 mcg), sulphatriad (S3-300 mcg), and tetracycline (TE-30 mcg) were placed on agar plates (strength of antibiotics are written in bracket). The Petri plates were then incubated at 37 °C for 18 h and inhibition zones (IZ) were measured using Antibiotic Zone (mm) Scale-C (PW297, HiMedia, India).

Physio-biochemical characterization of the isolate

Physio-biochemical characterizations were performed following standard protocol (Pelczer 1957). Biochemical properties like extracellular enzyme production (catalase, amylase, protease and lipase), substrate utilization tests (such as citrate, tributyrin, and olive oil) were performed. Utilization of carbohydrate sources like D-glucose, fructose, sucrose, lactose, xylose, ribose, and galactose were tested. Optimal growth under different pH (2–11), salt concentration 1–16% NaCl and temperature tolerance were determined through thermal death point analysis, according to previously described methods (Holding and Collee 1971).

Phenotypic characterization by microscopic study

After screening with MTC value of $FeSO_4$ and antibiotic sensitivity test, the selected bacterial isolate i.e. BRTN was initially characterized for cell shape, size, and Gram characteristic using a bright field microscope (Leica DM1000, Germany) at 40 × magnification; and a fluorescence microscope (Leica DM1000, Germany) at 40 × after staining with 4′,6-diamidino-2-phenylindole (DAPI) and observed under a blue filter (Hannig et al. 2007). Surface morphology was examined using Scanning Electron Microscopy (SEM, Jeol, JSM 6390 LV, Japan), while and the internal structures were analysed by Transmission Electron Microscopy (TEM, JEOL; JEM 1400 plus), following standard protocols (Prior and Perkins 1974).

Whole genome sequencing, assembly, annotation, and phylogenetic analysis of BRTN

Genomic DNA of a 24 h grown BRTN strain was isolated using Zymo research fungal/bacterial DNA mini prep kit,

USA (D6005) by following manufacturer's instruction. The quality and quantity of the DNA were assessed using NanoDrop 1000 spectrophotometer (Thermo Scientific, USA). For optimal resolution, genomic DNA was analyzed by agarose gel electrophoresis using a 1.0% agarose gel matrix. The sequencing was done with high throughput sequencer Illumina Miseq (Illumina, USA). The library was prepared following Illumina TrueSeq DNA PCR-free HT library preparation kit. For quality check of raw paired-end Fastq reads, FastQC software (Andrews 2010; Kircher 2011) was used followed by trimming of low- quality bases using Trimmomatic software (Bolger et al. 2014). The resulting sequence data was assembled using SPAdes (Bankevich et al. 2012), VelvetOptimizer (Zerbino and Birney 2008), and ABySS (Jackman et al. 2017). Comparative evaluation of the assemblies was carried out using quality assessment tool (QUAST) (Mikheenko et al. 2023). Type (Strain) Genome Server; TYGS (Meier-Kolthoff and Göker 2019) was used for further analysis of QUAST results with the highest N50 length. Finally, contigs were ordered using progressiveMauve to obtain the draft assembly of the BRTN genome. The assembled contigs were then annotated using Prokka software (Seemann 2014), Rapid Annotation System Technology (RAST) (Aziz et al. 2008), and National Centre for Biotechnology Information (NCBI) pipeline (https://www.ncbi.nlm.nih.gov; accessed on 02.10.2024). The phylogenetic analysis was carried out using TYGS server and Ez BioCloud (https://www.ezbiocloud.net/.; accessed on 10.10.2024).

Visualization of genomic features of strain BRTN

The visualization for genomic features of BRTN was carried out using Proksee server (Grant et al. 2023) and progressiveMauve webserver (Darling et al. 2004); accessed on 10.10.2024. For prediction of genomic islands within the genome of BRTN, IslandViewer 4 (https://www.pathogenomics.sfu.ca/islandviewer/; accessed on 15.11.2024) was used. Prediction of protein-encoding, rRNA, and tRNA genes, analyses of functional genes, and projection of subsystems were analyzed by RAST server. Whereas, Comprehensive Antibiotic Resistance Database (CARD) (https://card.mcmaster.ca/; accessed on 21.11.2024) (McArthur et al. 2013; Raphenya et al. 2022) and VFDB web tools (https://www.mgc.ac.cn/VFs; accessed on 21.11.2024) were used to check antibiotic resistant genes (ARGs) and virulence status of BRTN, respectively.

Core, accessory, and unique genome analysis

The BRTN genome was analyzed using Spine and AGEnt (Ozer et al. 2014) tool. Reference genome sequence of FASTA formats was uploaded to the programming software Spine (http://vfsmspineagent.fsm.northwestern.edu/cgi-bin/spine.cgi; Accessed on 30.03.2024) to find out the core, accessory, and unique genes present in BRTN.

In silico molecular analysis of SUF system as a potent drug target

Subtraction, screening, and identification of essential proteins

In this in silico study, the Database of Essential Genes (DEG) (http://origin.tubic.org/deg/public/index.php; accessed on 21.11.2023) was used to identify genes within *Bacillus* sp. BRTN genome that are essential to cope with harsh conditions (Zhang et al. 2004; Luo et al. 2021; Gorityala et al. 2024). The corresponding essential protein sequences were subjected to BLASTp analysis against the *Homo sapiens* proteome, using an expectation value (*e*-value) of 10^{-3}. For subsequent analysis, only SUF proteins without human homolog were considered. The UniportKB database was used to retrieve homologous sequences of the SUF family proteins through BLASTp analysis.

Determination of subcellular location of the selected proteins

To anticipate the location (i.e., whether extracellular, intracellular or membrane bound) of the SUF proteins (SufB, SufC, SufD, SufE, IscR, and PaaD-like protein, ApbC, Cysteine desulfurase), web server PSORTb (Yu et al. 2010) and CELLO v.2.5 (http://cello.life.nctu.edu.tw/cgi/main.cgi) were accessed on 17.01.2024 (Jones et al. 2022).

Primary analysis of physico-chemical parameters and structure of the selected proteins

The primary physico-chemical parameters of the proteins such as number of amino acids, theoretical isoelectric point (pI value), grand average of hydropathicity (GRAVY), molecular weight, aliphatic index (AI) and instability index (II) were computed through ExPASy- ProtParam (https://web.expasy.org/protparam/ accessed on 15.04.2024).

Analysis of secondary structure of SUF protein

The protein secondary structures (% of α-helix, β turn and β sheets) were predicted by Self Optimized Prediction Method with Alignment (SOPMA) server (https://npsa-prabi.ibcp.fr/cgibin/npsa_automat.pl?page=/NPSA/npsa_sopma.html; accessed on 17.04.2024) (Geourjon and Deleage 1995).

Homology modeling and structural validation

At the beginning, amino acid sequences of eight SUF proteins were retrieved and three-dimensional structures were generated using SWISS-MODEL (https://swissmodel.expasy.org/interactive) server. The best structural models were selected based on GMQE values (>0.6), QMEAN score (closest to zero) and higher sequence identity with the selected template. Predicted structures of the models were validated using the SAVESv6.1 server (https://www.doe-mbi.ucla.edu/saves/) and MolProbity (https://molprobity.biochem.duke.edu/). Validation metrics included ERRAT scores, clash scores, Ramachandran plots, rotamer outliers, backbone geometries and torsion angles. Additionally, the ProsSA-web server (https://prosa.services.came.sbg.ac.at/prosa.php) was used to analyze the Z-score distributions. All servers were accessed during 15.02.2025 to 28.02.2025.

Compound selection for targeting SUF proteins

Potential SUF protein inhibitors were retrieved from ChEMBL (https://www.ebi.ac.uk/chembl/), BindingDB (https://www.bindingdb.org/rwd/bind/as.jsp), and PubChem (https://pubchem.ncbi.nlm.nih.gov/; accession date 17.02.2025) databases. Specific protein sequences were used for target specific ligand selection. Compounds were evaluated and selected based on favorable physiochemical properties (molecular weight < 500 Da, LogP < 5.0, hydrogen bond donors ≤ 5.0, and hydrogen bond acceptors ≤ 10 (Gorityala et al. 2024). The 3D structures of the selected compounds were downloaded in .sdf format from PubChem. Ligand selection also considered bioactivity data such as IC_{50}, K_i, MIC, and EC_{50} values, corresponding to the matched protein targets. Compound 882 and D-cycloserine (CHEMBL1539876) were taken as a positive control due to their previously reported inhibitory effects on Fe–S cluster biogenesis and cysteine desulfurase activity, respectively (Choby et al. 2016; Garcia et al. 2022). Additionally, a series of fluroquinolones, ranging from 1st to 4th generation antibiotics, were selected to compare their efficacy and binding affinity toward SUF proteins. All the selected compounds were prepared for docking using Avogadro (https://avogadro.cc/) tool by adding hydrogen atoms. Geometries of the selected compounds were optimized using a force-field energy minimization algorithm. Protein structure was also purified by removing water molecules and previously attached ligands using BIOVIA Discovery Studio. All database and tools were accessed during 15.02.2025 to 28.02.2025.

Molecular docking and protein–ligand interactions

Molecular docking was performed using CB-DOCK2 (Cavity-detection guided blind docking) server (Liu et al. 2022). The docking workflow involved automatic binding pocket prediction followed by AutoDock Vina-based docking simulations. For each SUF protein–ligand pair, multiple binding pockets were generated, and the complex with the lowest Vina score (indicates the highest binding affinity in kcal/mol) was selected for further analysis.

The 2D interaction diagrams of SUF protein–ligand complexes were generated using BIOVIA Discovery Studio to identify the interacting amino acid residues. Docking results were compared with those of the positive control inhibitors to evaluate the potential of newly screened compounds. All servers were accessed from 25.02.2025 to 10.05.2025.

Results and discussion

Sampling and study area

During the sample collection in June 2022, the temperature of sampling point was 37°C and pH of the mud was 7.0. However, at the mud emergence site (a small hole like structure, Fig. 1c), the temperature was around 40–50°C (Fig. 1b). The mud or sediment sample exhibited a semi-liquid consistency, grayish colour, and slightly slimy texture.

Physicochemical analysis of the mud sample

Elemental analysis showed the presence of carbon (0.402%), hydrogen (0.134%), nitrogen (~0.009%), and sulfur (0.039%) with a high C/N ratio of 45.205. FTIR spectra (Fig. 2a) showed a strong band at 1022.27 cm^{-1} which is the asymmetric stretching vibrations of Al–O/Si–O bonds, indicating the presence of Si and Al in the mud. These elements are the second and third most abundant elements in Earth's crust, respectively (Harris 1993). A weak absorption band around 794.07 cm^{-1} corresponds to stretching and bending vibration of OH^- and H–O–H groups, likely due to weakly bound water molecules absorbed on the surface or trapped within geopolymeric products (Krivoshein et al. 2022). Strong stretching at 1793 cm^{-1} and 1870 cm^{-1} of acid halides were observed, indicating the presence of chlorinated halogen compounds. A medium intensity bending vibration of alkane methyl group at 1427.32 cm^{-1} was detected. While C=C stretching of disubstituted alkenes appeared at 1635.64 cm^{-1}. Additional, C-O stretching vibration were detected at 1870.95 and 1793.80 cm^{-1}. ICP-AES analysis (Fig. 2b) detected a high concentration of Fe (57.23 mg L^{-1}), Mg (14.59 mg L^{-1}), Na (11.38 mg L^{-1}), Ca

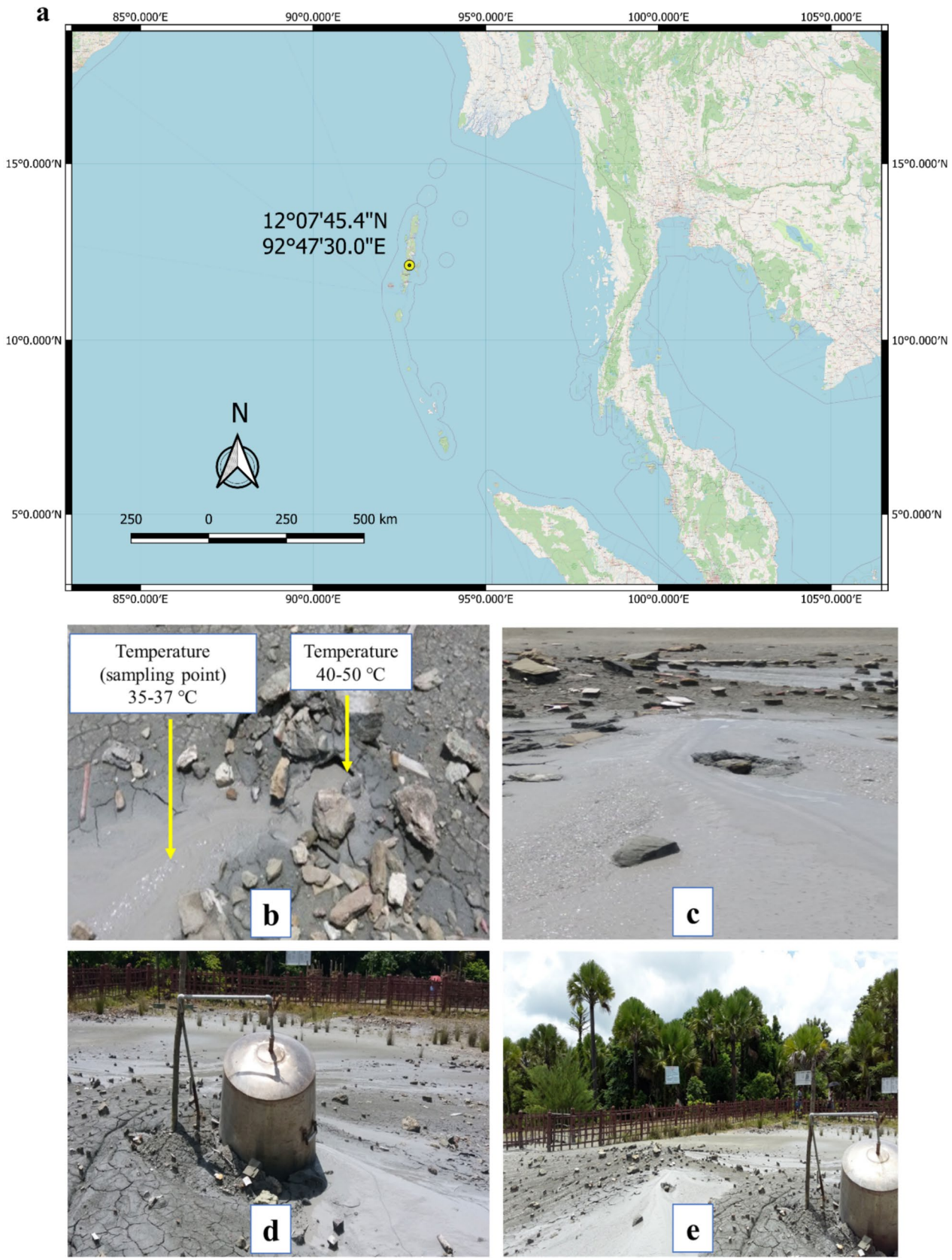

Fig. 1 **a** Geographic coordinates of the sampling area at Baratang mud volcano, Andaman and Nicobar Islands, generated using QGIS software; **b** sampling point and mud volcano vent (from which mud was oozing out); **c** sediment of the mud; **d.** and **e.** broad view of the sampling area

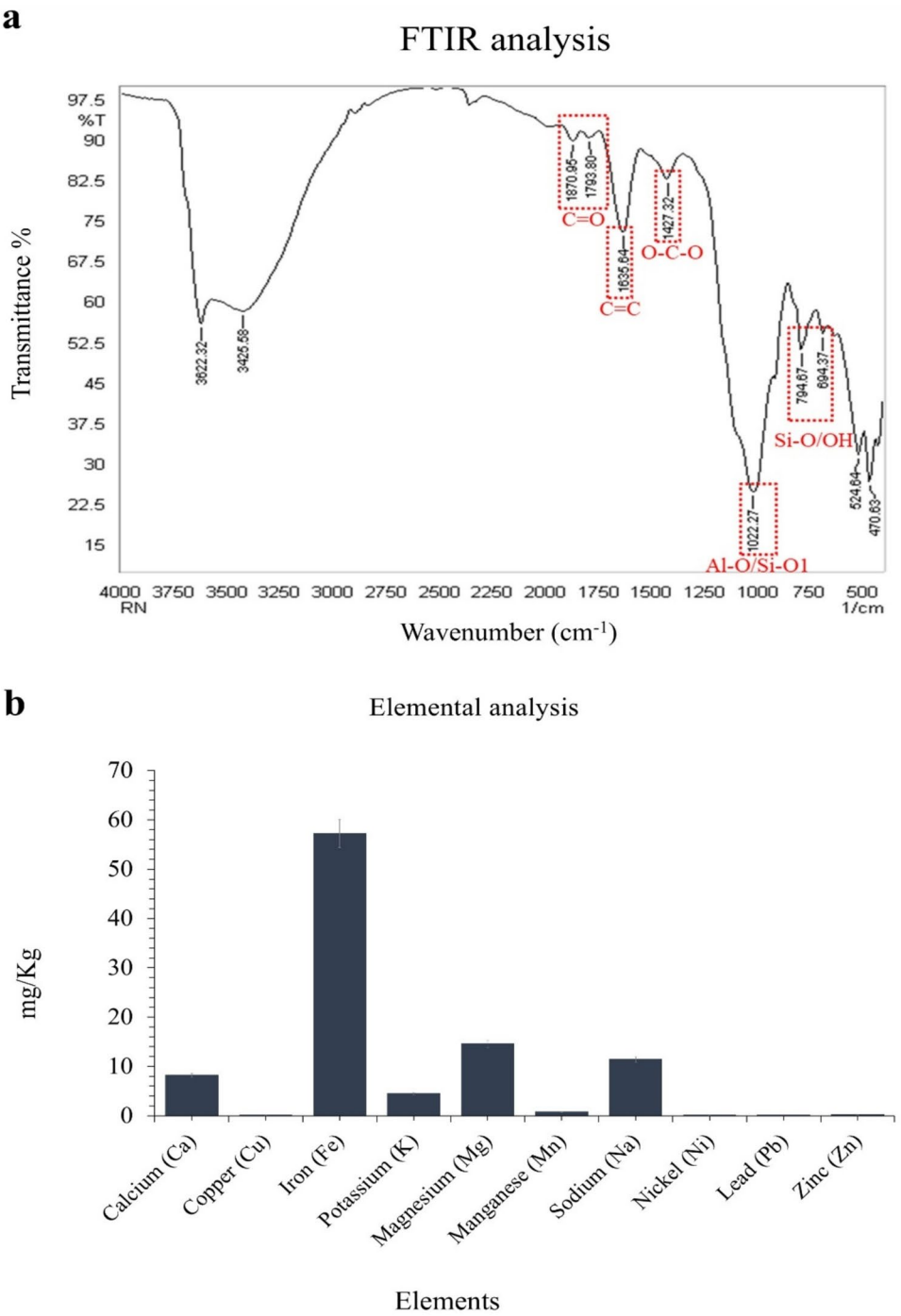

Fig. 2 **a** FTIR spectrum showing probable functional groups in the mud sample, and **b** elemental composition of the mud sample from the Baratang mud volcano located at the Andaman and Nicobar Islands, India

(8.201 mg L^{-1}), and K (4.452 mg L^{-1}) in the mud sample. These metal ions are fundamental to maintain both microbial physiology and the unique nature of geological environment of mud volcanoes, offering insight into microbial survival and with the environmental interactions (Galera-Laporta et al. 2021). They can function as co-factors essential for enzymes activity as well as play roles in electron transfer, membrane transport, cell wall stabilization, osmoregulation pH homeostasis, enzyme activation, and signal transduction. Collectively, these cellular features support microbial communities to adapt and survive in harsh environmental condition (Hemkemeyer et al. 2021; Stautz et al. 2021; Wendel et al. 2022).

Isolation and screening of bacteria from mud sample

The collected mud sample was serially diluted up to 10^{-4} dilution and spread plating was performed on starch casein agar and minimal salt agar media. A total of 10 morphologically distinct bacterial colonies were isolated. Further LB media was used for subculture among which the BRTN strain was selected based on its ability to tolerate the highest iron tolerable concentration (>600 mg L^{-1} of $FeSO_4$) using MSM media.

Maximum tolerable concentration (MTC) of $FeSO_4$

Among the analyzed elements in the mud sample, Fe was the most abundant metal, with the concentration of 57.23 mg L^{-1}. Therefore, the MTCs of $FeSO_4$ for the bacterial strains were determined applying the described methods by Shylla et al. (2021). The experimental evidence showed that, BRTN showed the highest MTC value at 600 mg L^{-1} FeSO4 (Fig. 3e), while other strains showed MTCs like BRTN2 at 500 mg L^{-1}, BRTN3 400 mg L^{-1}, BRTN4 400 mg L^{-}1, BRTN5 300 mg L^{-1}, BRTN 9 500 mg L^{-1}, BRTN 10 600 mg L^{-1}, BRTN11 500 mg L^{-1}, BRTN12 500 mg L^{-1}, BRTN13 600 mg L^{-1} (Fig. S1). Strain BRTN showed the highest Fe tolerance and had the best capability to alleviate iron-induced toxicity. Iron is an essential micronutrient and functions as a co-factor in various biological process, including enzymatic activity, cellular metabolism, electron transport, and redox reaction (Esquilin-Lebron et al. 2021; Klebba et al. 2021; Vats et al. 2022). Since, low concentrations of Fe may promote bacterial growth, excessive levels may have toxic effects on organisms (Lankford and Byers 1973; Pronk and Johnson 1992; Andrews et al. 2003; Cornelis et al. 2011). Supporting this theory, BRTN demonstrated growth across a wide range of $FeSO_4$ concentration, from 10–600 mg L^{-1}. Notably, lower concentration of Fe enhanced bacterial growth, suggesting that BRTN utilizes Fe as a micronutrient to support its metabolic functions. Optimal growth under laboratory conditions was observed at 200 mg L^{-1} $FeSO_4$, beyond which growth gradually declined, with increasing $FeSO_4$ concentrations. Finally, growth was not evident after 600 mg L^{-1}, possibly that point might exerted toxicity on its metabolism due to oxidative damage induced by Fenton reaction (Fig. 3e). Other studies have reported that strains of *Bacillus zhangzhouensis*, *Bacillus cereus*, *Bacillus altitudinis*, *Brevibacterium frigoritolerans*, which tolerate up to 550 mg L^{-1} $FeSO_4$, while *Bacillus toyonensis*, *Rhodococcus hoagii*, *Lysinibacillus fusiformis*, *Lysinibacillus mangiferihumi* are reported to tolerate up-to

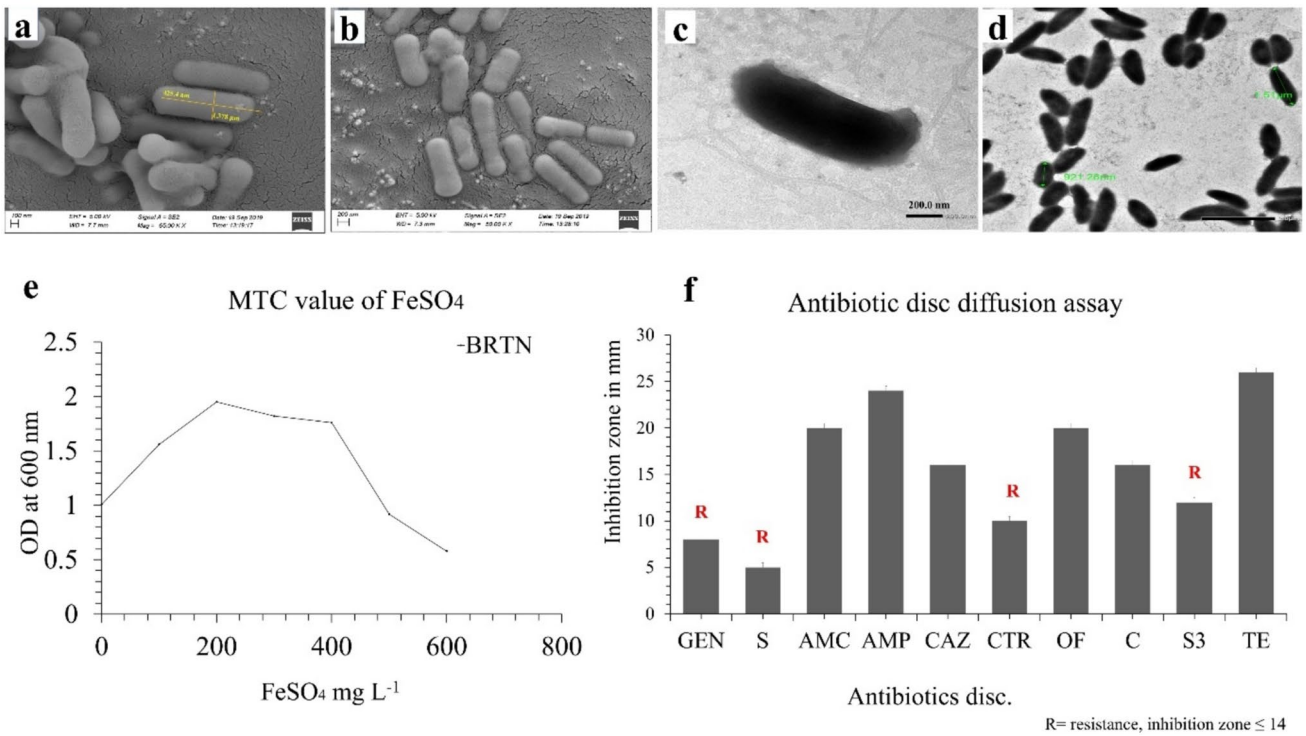

Fig. 3 **a**, **b** Micrographs of scanning electron microscopy (SEM), (size of the bacterium was 425.4 nm in width and 137.8 nm in length, scale bar: 200 nm); transmission electron microscopy (TEM) showing morphology of BRTN, (scale bar: 200.0 nm) (**c**), (length of cells 921. 26 nm and 151.0 nm, scale bar 20.0 µm) (**d**); **e** maximum tolerable concentration (MTC) value of the isolates in different concentration of $FeSO_4$; **f** antibiotic sensitivity test by using disc diffusion assay (AMC-amoxyclav, AMP-ampicillin, CAZ-ceftazidime, CTR-ceftriaxone, GEN-gentamicin, OF-ofloxacin, C-chloramphenicol, S-streptomycin, S3-sulphatriad, TE-tetracycline,≤14-resistance.)

400 mg L^{-1} $FeSO_4$ (Alnaimat et al. 2017; Jinal et al. 2019). These results support the fact that iron tolerance may vary greatly across species or strain to strain.

Antibiotic sensitivity test

The selected bacterial isolates were subjected to commercially available antibiotics for the sensitivity profiling. It was found that, BRTN showed lowest sensitivity to most of the tested antibiotics, and resistance to gentamicin (GEN), streptomycin (S), ceftriaxone (CTR), and sulphatriad (S3) antibiotics (Fig. 3f). Whereas, other strains such as BRTN12, BRTN 13 showed highest sensitivity towards the applied antibiotics (Fig. S2). The resistance pattern was determined on the basis of clinical laboratory standard institutes (CLSI) (https://www.nih.org.pk/wp-content/uploads/2021/02/CLSI-2020.pdf). Based on the criteria of CLSI 2020, if any bacterium shows an inhibition zone with a diameter of≤14 mm, should be considered as resistant strain. Hence, BRTN was able to resist antibiotics like GEN, S, CTR, and S3.

Earlier, scientists had been primarily focused on the mechanisms of antibiotics that inhibit key bacterial processes, such as interference with cell wall synthesis (e.g., β-lactam antibiotics penicillin derivatives, cephalosporins, monobactams and carbapenems), inhibition of protein synthesis (e.g., aminoglycosides antibiotics- neomycin, streptomycin and kanamycin; tetracycline antibiotics), inhibition of nucleic acid synthesis (e.g., trimethoprim antibiotics-Sulphonamides), disruption of cell membrane function (e.g., aminoglycosides antibiotics- neomycin, streptomycin and kanamycin), and inhibition of metabolic pathways (e.g., fluoroquinolones-inhibition of DNA metabolism) (Davies 1990; Dowling et al. 2017; Baran et al. 2023). However, the alarming rate of multidrug resistant in bacterial strains has prompted to explore alternative antibacterial strategies, such as modification of virulence factors, oxidative stress response genes, transporters and efflux pumps, cell division machinery, and chaperon proteins (Banerjee et al. 2019; Vaishampayan and Grohmann 2022). These emerging approaches are often grounded in the understanding that many bactericidal antibiotics exert their effect by inducing oxidative stress, thereby generating reactive oxygen species (ROS) that damage bacterial components. Interestingly, in this study, strain BRTN showed the ability to tolerate high concentration of $FeSO_4$ (600 mgL^{-1}), and concurrently exhibited resistance to several bactericidal antibiotics including Gentamycin, Streptomycin (group- Aminoglycosides), Ceftriaxone (group-β-lactam; class-cephalosporine), and Sulphatriad (Sulphonamide class). These antibiotics are known to promote oxidative stress in bacteria by enhancing citric acid cycle rate and electron transport chain flux, leading to generate reactive oxygen species (ROS), such as hydroxyl radicle, as a direct killing mechanism. Similarly, high Fe concentrations can also induce ROS formation through the Fenton reaction. This suggest that strain BRTN may employ adaptive counter strategies to withstand oxidative stress arising from both iron overload and antibiotics exposure (Liu et al. 2023). To investigate this, an in silico study was performed (discussed in later sections) for further confirmation. Moreover, this finding may support the co-selection theory of heavy-metal and antibiotic-resistance. Co-selection facilitated by interventions of chromosomal or extra chromosomal (environmental) factors, promoting both co-resistance and cross resistance (Pal et al. 2015; Halder et al. 2022; Vats et al. 2022). Heavy metals are strictly regulated within bacterial cell, while trace amounts function as essential micronutrients, and elevated concentrations are toxic. To survive, bacteria must either excrete toxic ions, synthesize protective components, or activate alternative metabolic pathways to maintain cellular homeostasis. This selection pressure may drive the evolution of metal tolerance and antibiotic resistance concurrently, contributing to bacterial adaptation in extreme environments.

Polyphasic characterization of the isolates

The colony morphology of maximum isolates was circular in shape, only BRTN3 showed wavy appearance. All isolates were nonmotile in nature. Physiochemical characterization for all the isolates is represented in Table 1. Particularly the 24 h old colony of isolate BRTN appeared round, with a diameter of~0.4 mm, a dry texture, and white coloration. Microscopic analysis confirmed that strain BRTN was a rod shaped (Fig. 3a, b), Gram-positive flagellated bacterium (Fig. 3c, d). A series of biochemical tests were performed for partial identification of the isolate (Table 1). All the isolates showed positive result to catalase and negative to citrase. While, only BRTN11 produced lipaseextracellularly. The optimum growth temperature for BRTN was 37 °C, but it can survive in temperatures up to 80 °C, as determined by thermal death point. Whereas, BRTN2 and BRTN10 showed higher thermotolerance, with thermal death point of 100 °C and 90 °C respectively. All the isolate exhibit halotolerance, with optimal growth at 4% NaCl concentration. They can tolerate salt levels exceeding 10%, with visible growth observed at concentrations up-to 14–16% NaCl. All the bacterial isolates showed observable growth in alkaline pH. Similar extremophilic traits have been reported in thermotolerant *Bacillus* sp., halotolerant *Arhodomonas* spp. and *Haloferax* sp. MSNC14, and alkaline protease producing *Bacillus safensis* (alkaline protease) (Rekik et al. 2019; Matkawala et al. 2021; Benítez-Mateos and Paradisi 2023; Aqel et al. 2024). Additionally, BRTN produced several extracellular enzymes, including amylase,

Table 1 Polyphasic characterization including colony morphology, extracellular enzyme production, salt concentration tolerance by the strain BRTN

	Bacterial sample									
	BRTN	BRTN2	BRTN3	BRTN4	BRTN5	BRTN9	BRTN10	BRTN11	BRTN12	BRTN13
Colony morphology										
Size (cm)	0.4	0.4	0.4	0.4	0.5	0.4	0.3	0.2	0.5	0.4
Form	Circular	Circular	Wavy	Circular	Circular	Circular	Circular	Circular	Circular	Wavy
Margin	Entire	Regular	Irregular	Irregular	Entire	Entire	Entire	Regular	Entire	Irregular
Texture	Dry	Sticky	Dry	Moisturize	Dry	Sticky	Moisturize	Sticky	Dry	Moisturize
Pigmentation	White, Non-pigmented	Creamy	Non-pigmented	Yellowish	Creamy	Non-pigmented	Yellowish	Off-white	White, Non-pigmented	Pinkish
Optical property	Opaque	Translucent	Transparent	Opaque	Opaque	Transparent	Opaque	Translucent	Translucent	Opaque
Motility	Motile	Non-motile	Motile	Non-motile	Non-motile	Motile	Non-motile	Non-motile	Motile	Motile
O_2 Utilization	Aerobic	Aerobic	Aerobic	Aerobic	Aerobic	Aerobic	Aerobic	Aerobic	Aerobic	Aerobic
Enzyme production assay										
Catalase	+ve	+ve	+ve	+ve	+ve	+ve	+ve	+ve	+ve	+ve
Amylase test	+ve	+ve	+ve	+ve	+ve	+ve	+ve	-ve	+ve	-ve
Protease test	+ve	−ve	−ve	−ve	−ve	−ve	−ve	+ve	−ve	−ve
Esterase test	−ve	−ve	−ve	−ve	−ve	−ve	−ve	+ve	−ve	−ve
Lipase test	−ve	−ve	−ve	−ve	−ve	−ve	−ve	+ve	−ve	−ve
Xylanase test	+ve	+ve	+ve	+ve	+ve	−ve	−ve	+ve	−ve	−ve
Cellulase test	+ve	+ve	+ve	+ve	+ve	−ve	−ve	−ve	−ve	-ve
Carbohydrate utilization test										
Mannose	−Ve	+Ve	−Ve	−Ve	+Ve	+Ve	+Ve	+Ve	−Ve	−Ve
Sucrose	−Ve	+Ve	+Ve	−Ve	−Ve	−Ve	−Ve	−Ve	+Ve	−Ve
Xylose	−Ve	−Ve	−Ve	−Ve	+Ve	−Ve	+Ve	−Ve	+Ve	−Ve
Fructose	+Ve	+Ve	−Ve	+Ve	+Ve	+Ve	−Ve	−Ve	+Ve	+Ve
Lactose	−Ve	−Ve	−Ve	−Ve	+Ve	−Ve	+Ve	+Ve	−Ve	+Ve
Galactose	−Ve	−Ve	+Ve	−Ve	+Ve	−Ve	−Ve	+Ve	−Ve	−Ve
Ribose	−Ve	−Ve	+Ve	−Ve	+Ve	−Ve	+Ve	+Ve	−Ve	+Ve
D-glucose	+Ve	−Ve	+Ve	+Ve	−Ve	+Ve	−Ve	−Ve	+Ve	+Ve

Remarks: (in case of enzymes, +ve = can produce, −ve = cannot produce; In case of carbohydrate, +Ve = can utilize, −Ve = can-not utilize)

protease, catalase, xylanase, and cellulase, although it was unable to utilize substrate such as tributyrin and olive oil (Table 1). Regarding carbon source utilization, BRTN was capable of metabolizing glucose and fructose as primary carbon sources.

Whole genome sequencing, assembly, annotation and phylogenetic analysis of BRTN

The whole genome sequencing of BRTN was performed to predict its genomic features and taxonomic status through different web tools. RAST annotation suggested its genome size of approximately 3.4 MB and a GC content of 35.9%. The assembly consisted of 32 contigs with a N_{50} value of 9,63,689 bp. A total of 3,514 protein coding genes were identified and categorized into 290 subsystems. Additionally, 187 pseudogenes were also noticed. The genome also contained 97 tRNA genes, 14 5S rRNA genes, 8 16S rRNA genes, 14 23S rRNA genes, and 5 non-coding RNA (ncRNA) genes. Whole genome based phylogenomic analysis using TYGS indicated close proximity with *Bacillus anthracis* (Fig. 4a). Whereas, comparative analysis based on average nucleotide identity (ANI) and 16S rRNA gene sequence similarity (via the EZBiocloud platform), revealed less than 93% similarity with *Bacillus paranthracis (GenBank: PV125264)* (https://www.ezbiocloud.net/). Due to this low similarity, the BRTN strain has been designated as *Bacillus* sp. (NCBI accession number: PRJNA762599, BioSample: SAMN21399064).

Visualization of genomic features of strain BRTN

RAST analysis (Fig. 4b, c) showed the metabolism of amino acid and derivatives subsystems occupied largest number of genes (229) followed by protein metabolism (153); carbohydrate metabolism (145); cofactors, vitamins, prosthetic groups, pigment (113); and so on. It had many stress response genes (29) including multidrug transporter

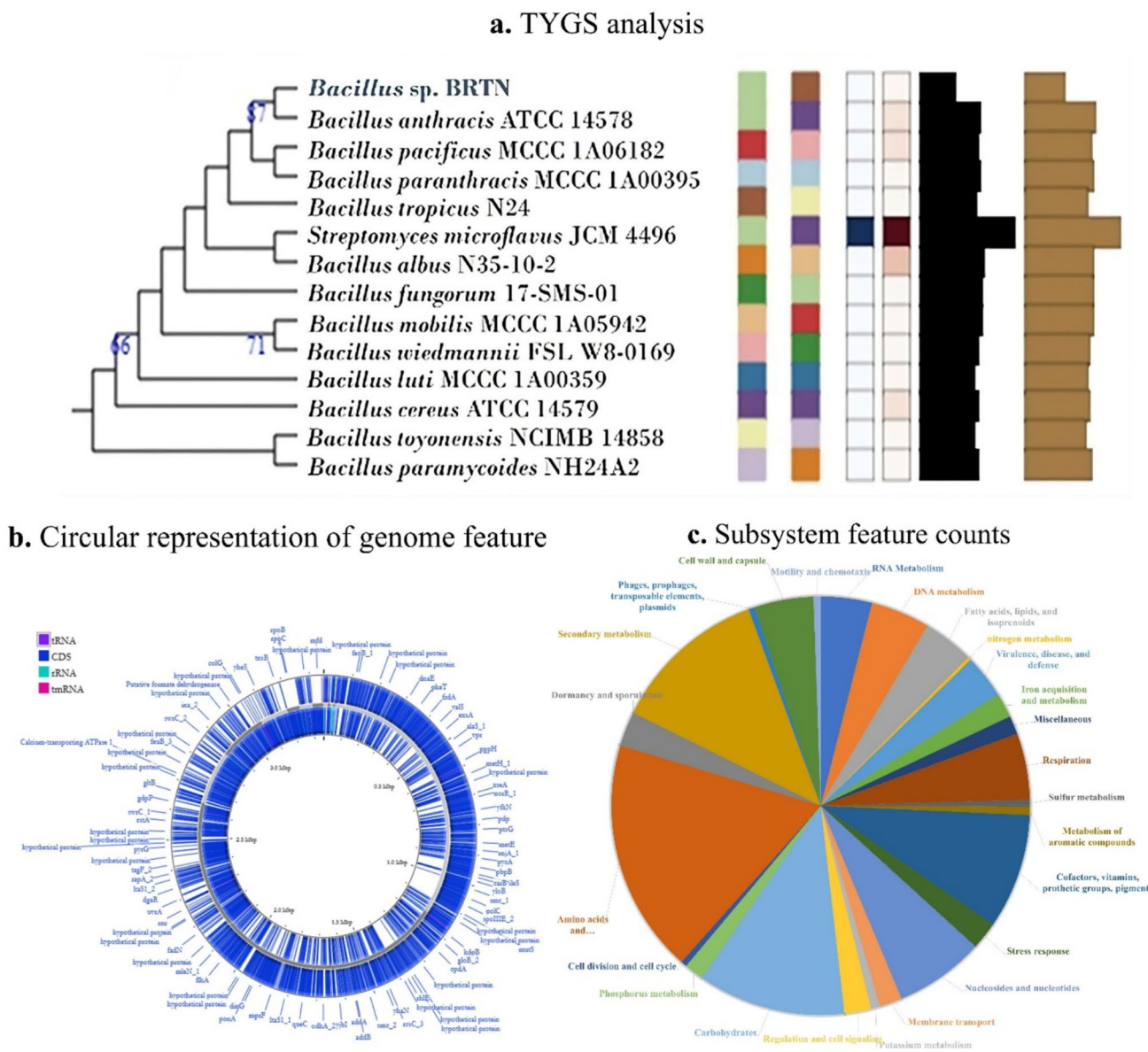

Fig. 4 **a** Strain identification using the TYGS server showing phylogenetic relationships; **b** circular genome map of BRTN displaying annotated genomic features; **c**. subsystem feature distribution generated through RAST annotation

(*Bcr*/*cfiA*), MDR cluster, DNA gyrase subunit A and B, MATE family MDR pump, acriflavine resistance protein (*AcrB*); some heavy metal and multi metal resistance protein; transporter genes such as *CzCD, Trcd, MerR, HmrR, Cia, Csa* and ATPase pump etc. It also contained Fe transporter genes like *PitA, PitC, PitD,* IsdACDEF operon, siderophore protein (YuiI), Fe uptake system, siderophore binding protein FeuA, FeuB, FeuC, petrobactin (PB_PBP, PB_ABP, PB_PPI), ferric uptake regulator protein i.e., FUR, some oxidative stress regulator proteins involving superoxide dismutase, PerR etc. (Fig. 4b, c). The genomic feature of BRTN represented many genes including Fe–S cluster biogenesis machinery i.e., SUF system. This SUF system includes sufABCDES operon (genes like *sufB*, *sufC*, *sufD*, *sufE*, *sufS*, Paad-like protein, systeine desulfurase, and *sufR*) among which some specific components play crucial roles in Fe–S cluster formation (Garcia et al. 2022). SUF system encoded proteins play important roles in bacterial survival and metabolism under oxidative stress and Fe limited condition. Oxidative stress on microorganisms could also be generated due to iron toxicity, antibiotic stress or other adverse conditions (Le Touati 2000; Ezraty et al. 2013; Guillouzo and Guguen-Guillouzo 2020; Elchennawi and Ollagnier de Choudens 2022; Liu et al. 2023). In this study, reduction of bacterial growth under high Fe concentration and antibiotic treatment may also be associated with oxidative stress.

While, Fe tolerance as well as antibiotic resistance could be directly or indirectly related to SUF system. The study of SUF proteins is significant for several reasons. Various studies have demonstrated that the SUF system may function as the sole pathway for Fe–S cluster biogenesis in many bacterial species (Dussouchaud et al. 2024); also in our computational study, through RAST and whole genome sequence analysis we also evaluated that BRTN possesses only SUF system as Fe–S cluster biogenesis machinery. The genes involved in Fe–S cluster formation are often expressed during the lag phase of bacterial growth (Rolfe et al. 2012). It is also known that elevated Fe concentrations during lag phase induce oxidative stress, which may, in turn, trigger the activation of the SUF operon to enhance bacterial defense mechanism and support growth during logarithmic phase. CARD database has identified a cluster of genes conferring glycopeptide resistance, indicated by the presence of van gene clusters (*vanT*, *vanW*, *vanY* from different clusters including vanB, vanF, vanG, vanI), all associated with antibiotic target alteration mechanism. Additionally, a macrolide resistant gene, *mphL* (macrolide phosphotransferase) was detected, conferring resistance via antibiotic inactivation (Supplementary file 2). The VFDB-based analysis of the strain BRTN revealed the presence of a restricted set of virulence-associated genes. These include *sph* and *hal*, which are interacted with host membrane, *ilsA* involved in iron acquisition (Daou et al. 2009), and the global regulators *papR* and *plcR*, known to control the expression of multiple virulence factors in *Bacillus* spp. (Pheepakpraw et al. 2025). In addition, *cheA* (chemotaxis regulator) was identified suggesting a possible role in host colonization (Supplementary file 2).

Genomic islands

A total of 3 Genomic Islands (GIs) of BRTN have been identified which covered only 2% of the genome. Genomic island-1 and 2 (GI-1 and 2) (Fig. 5a) harbored Tn7 superfamily genes. These are known to involve five transposons encoded genes *tnsABCDE*. Gene *tnsA* is responsible for making breaks in the 5′ end of DNA allowing excision via cut-and-paste mechanism, *tnsB* (large family of bacterial transposons), *tnsC* gene is encodes as regulatory proteins, *tnsD* directs the transcription into chromosome attTn7, whereas *tnsE* encourages horizontal transmission of mobile genetic elements. Many studies confirmed that Tn7 like elements play a major role in antibiotic resistance, non-ribosomal peptides synthesis, metal resistance, and bacterial CRISPR system (Peters et al. 2017). Another major transposon element belongs to DDE-type integrases/transposes/recombinase family, which has been also found to be integrated within BRTN genome. Transposons are mobile genetic elements that can move from one DNA to another to acquire new genes during transposition (Da Cunha et al. 2022). BRTN GI associated genes are usually related with DoxX family protein (function in Mycothiol recycling and cellular detoxification) (Nambi et al. 2015). GI-3 acquired SSpL (small acid soluble spore protein) plays an important role in DNA protection in dormant endospore against stress damage (Nerber and Sorg 2021). Additionally, the DHA2 family major facilitator superfamily (MFS) efflux transporter permease subunit, associated with antibiotic resistance, is also present in BRTN genome; these MFS efflux involves Fe efflux transport. DHA2 is a proton (H^+) pump that exchanges two H^+ with one substrate/drug (Pasqua et al. 2021). HLyD is also an important component of Cus-CFA multidrug efflux pump (Halder et al. 2022). Additionally, TetR/AcrR family transcriptional regulators (TFTRs) are also present in BRTN genome, which are reported to regulate virulence and resistance-related functions in bacteria (Colclough et al. 2019). IslandViewer 4 detected many hypothetical proteins within the GI and these proteins may play crucial roles in cellular metabolism and contribute to our understanding of mobile genetic elements acquired through horizontal gene transfer. Moreover, they could serve as candidates for uncovering novel stress response or regulatory mechanism. Interestingly, BLAST analysis between hypothetical proteins and SUF family proteins revealed that one hypothetical protein shared approximately 53% query coverage with IscR (iron-sulfur cluster regulatory protein). This finding suggests that certain hypothetical proteins may be involved in regulating core bacterial metabolic process or enhancing stress tolerance.

Core, accessory, and unique genome analysis

Genome analysis revealed that the total genome size of BRTN is 3,350,148 bp, of which 2,943,451 bp represented the core genome, 406,572 bp corresponded to the accessory genome, and only 125 bp was determined as unique genome part(Fig. 5b). Mobile genetic elements (MGEs) were frequently located within the accessory genome, contributing to genomic plasticity and adaptive functions. To further analyze these elements, the final sub-element file obtained through ClustAGE was subjected to WebMGA analysis for Cluster of Orthologous Groups (COG) functional categorization. ClustAGE clusters nucleotide sequences of accessory genomic elements (AGEs) to identify the minimal set of AGEs within a population and to determine their distribution across genome.

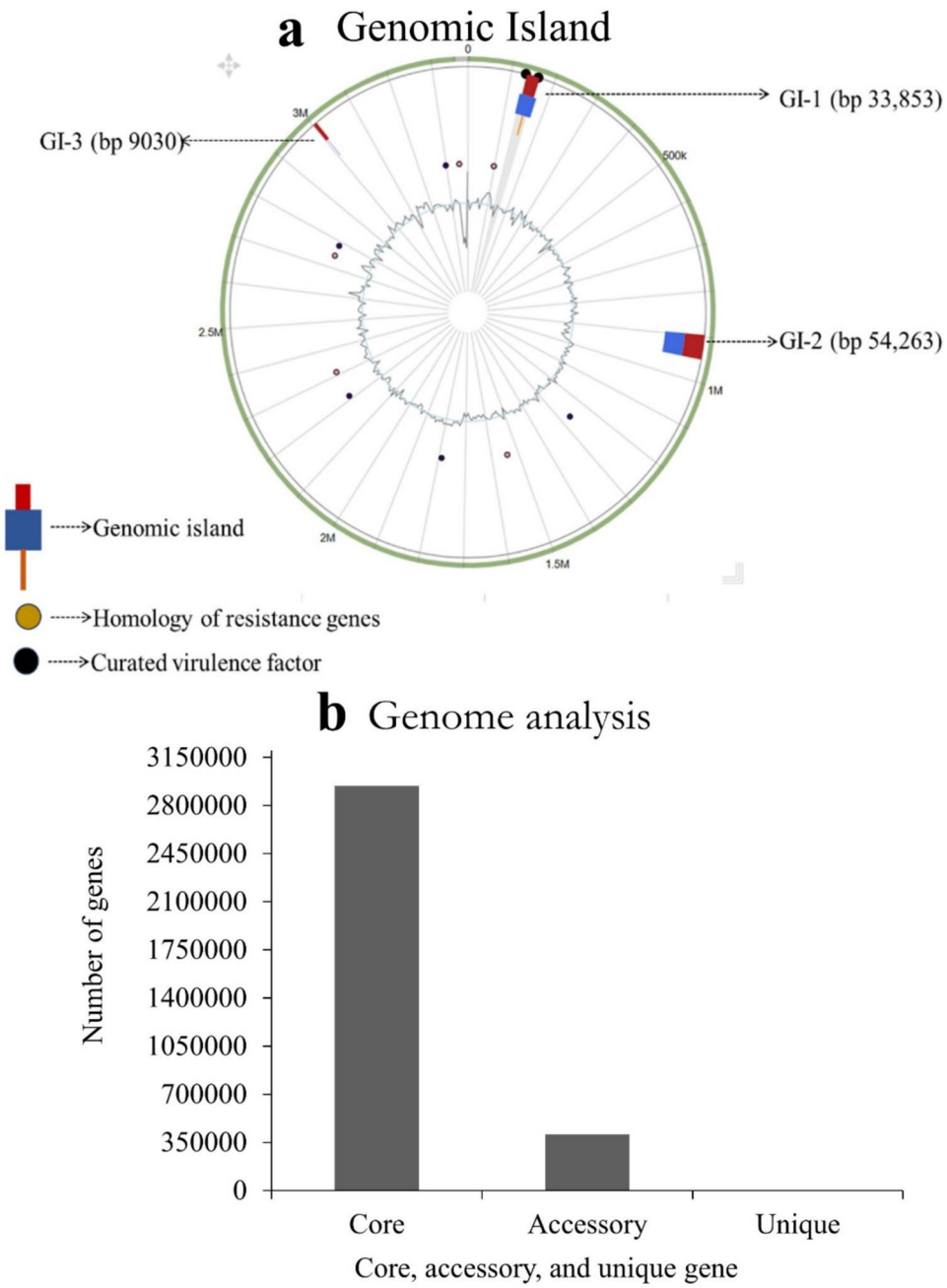

Fig. 5 **a** Genomic islands identified in the BRTN genome using IslandViewer 4; **b** Pangenome analysis showing core, accessory, and unique genomic regions. Overall, the accessory genomic content was relatively low in this strain.

In silico molecular analysis of the SUF system as a potent drug target

In this experiment, through RAST analysis, the presence of different metal and multidrug resistance proteins was observed. BRTN harbored a significant number of genes (Fig. 6a) like *sufB* (scaffold protein), s*ufC* (ATPase), *sufD* (scaffold protein), and *sufE2* (acceptor protein). The SUF family proteins are used to generate Fe–S cluster protein under stress conditions. *PaaD* and *IscR* (Fe–S cluster regulator) play potential role in Fe acquisition, metabolism and regulatory process. The cysteine desulfurase protein contains an active cysteine residue that participates in desulfuration and donate sulfur for the assembly of Fe–S clusters. The SufS/cysteine desulfurase is a pyridoxal 5′-phosphate (PLP)-dependent enzyme (Loiseau et al. 2003). PLP binds at catalytic site of L-cysteine and cuts C-S bond leading to the transfer of sulfur atom from L-cysteine to a conserved cysteine residue on SufS, resulting into the formation of a persulfide (–SSH) intermediate. This persulfide intermediate is then accepted by SufE, which enhance the activity of SufS, enabling it to catalyze the desulfuration of additional L-cysteine molecules to release more sulfur atoms. Further, SufE transfers the sulfur atom to SufB. Though

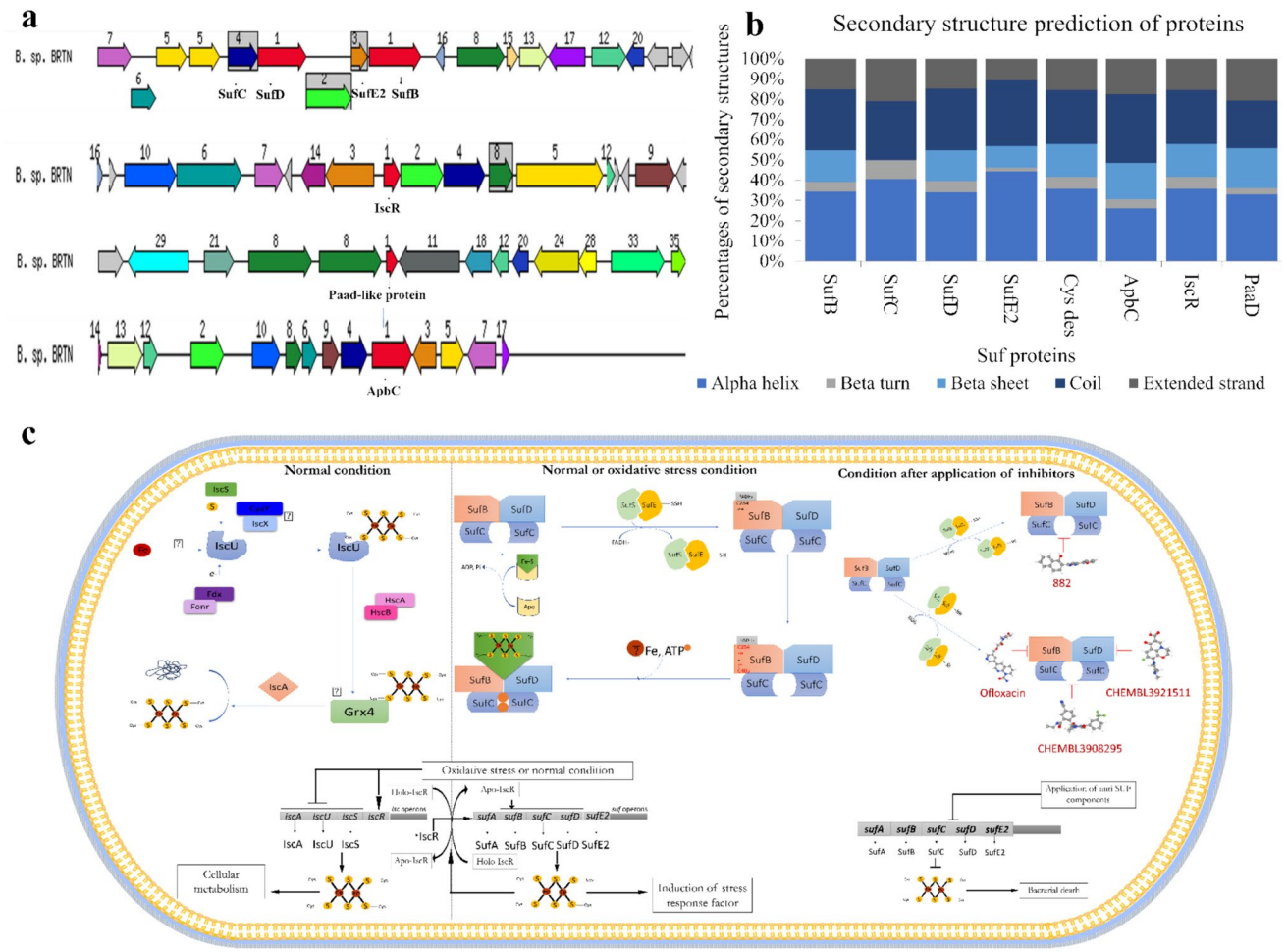

Fig. 6 **a** Genomic locations and predicted 3D structures of all SUF proteins; **b** predicted secondary structures of all SUF proteins; **c** schematic representation of the Fe–S cluster biogenesis mechanism in normal condition (1), normal and oxidative stress condition (2), condition after application of inhibitors (3), which results in cell death

the exact residue on SufB that receives persulfide remains unknown (Blahut et al. 2020). SufB provides a platform for the assembly of Fe–S cluster. It interacts with SufC and SufD forming a stable complex as a scaffold protein (Py and Barras 2010). SufC is a member of the ABC- transporter family and functions as a dimer, with one subunit binding to C-terminal helical domain of SufB and the other to the corresponding domain of SufD (Yuda et al. 2017). During ATP binding and hydrolysis process transient dimerization occurs, which triggers a conformational change at SufB-SufD interface, leading to the dissociation of anti-parallel β-sheets by exposing residues of SufBC405 and SufDH360 buried within the β-helix core domain on which the nascent Fe–S cluster assembly occurs (Yuda et al. 2017). After formation of Fe–S cluster it will be trafficked by SufA (sulfur mobilization protein) to the target apoprotein or the receiver apoprotein depending on environmental condition (Py and Barras 2010). For the Fe source, SufBCD system uses $FADH_2$ as a redox cofactor (Wollers et al. 2010). All this process is strictly regulated by IscR protein (thought as a pleiotropic regulator). BRTN also possessed Paad-like protein with DUF59 domain, which is a conserved domain but its function is still elusive. However, the SUF protein SufT, which contains the conserved DUF59 domain, is reported to localize with SufBC proteins and plays a role in Fe–S cluster assembly and maturation, particularly under conditions of elevated Fe–S cluster demand (Mashruwala et al. 2016). Scaffold proteins like ApbC and MRP-like proteins play a crucial role in [4Fe-4S] cluster assembly by facilitating the assemblage and delivery of these clusters to target proteins, acting as a platform for the process. This protein contains an ATP binding motif and a conserved CXXC motif involved in the binding of a bridging Fe–S cluster between monomers (Pardoux et al. 2019). Interestingly, these findings not only deepen the fundamental understanding of Fe–S cluster formation but also open doors for practical applications across multiple fields including therapeutic development. In this

section, in silico analyses of the SUF proteins will be carried out to identify the best protein for targeting drugs.

Subtraction, screening and identification of essential proteins

A computational subtractive genomics analysis was employed to identify essential, hypothetical, and non-homologous proteins. By implying DEG database, around 614 genes were identified as essential in the *Bacillus* sp. BRTN genome (Supplementary file 2). Among these, 177 were designated as hypothetical proteins. BLASTp of SUF proteins against *Homo sapiens* resulted with "NoHits" (indicating non-homologous sequences). For subsequent analysis, the non-homologous sequences, which exhibited no similarity with human host, were specifically chosen. Considering their essentiality, non-host nature, and involvement in vital pathways, all proteins in the SUF pathway hold promise as potential candidates for novel drug targets (Gorityala et al. 2024). Targeting any of these proteins could disrupt a pathway crucial for the pathogen's growth and survival. Inhibition of Suf proteins with specific inhibitors could impede Fe–S cluster assembly (Gorityala et al. 2024), thereby inducing a bactericidal effect through the Fenton reaction.

Determination of subcellular location of the selected proteins

Understanding the sub-cellular localization of a drug target is crucial for optimizing the drug's mode of action against specific target. Numerous examples in literature highlight cytoplasmic proteins as effective therapeutic targets due to their accessibility to drugs. The prediction of sub-cellular localization of Suf proteins was accomplished using computational tools, specifically PSORTb and CELLO. It was found that, these proteins are localized in the cytoplasm. The TMHMM value showed that these proteins did not possess transmembrane helices, further confirming their cytosolic location (Table S1). CELLO combines the sequence coding scheme analysis of amino acid composition, di-peptide composition, partitioned amino acid composition as well as physico-chemical properties of amino acids to determine the location of the proteins in the bacterial cells.

Primary analysis of physiochemical parameter and structure of selected proteins

Computational analysis of the physiochemical parameters of a protein gives a theoretical overview of the behavior and nature of the protein. Here, the SUF proteins were primarily characterized by basic physiochemical parameters such as amino acids compositions, pI, instability index, molecular weight, GRAVY, and aliphatic index (Table S2). It has been found that SufB, SufC, SufD, and SufE primarily are composed of basic amino acids, while cysteine desulfurase protein is dominated by acidic residues. In contrast, ApbC and IscR contain a balanced composition of both acidic and basic amino acids. SufB, SufC, SufD, SufE, Paad like protein, ApbC, IscR and cysteine desulfurase showed instability index of 33.84, 32.88, 24.14, 35.13, 37.57, 35.13, 51.10 and 28.71 respectively. Proteins with an instability index below 40 are considered as highly stable (Guruprasad et al. 1990; Sarkar et al. 2025).

Analysis of secondary structure SUF protein

SOPMA server (Geourjon and Deleage 1995) was utilized to predict secondary structures of the proteins (Figs. 5b, S1). Parameters included a window width of 17 and a similarity threshold of 8. Cysteine desulfurase was commonly rich in random coils, playing an important function in protein's flexibility and conformational changes. In addition, high percentage of α- helices were found in all the selected Fe–S cluster biogenesis proteins (Fig. 6b), which signified thermal resistance of proteins based on their intrinsic stability (Petukhov et al. 1997; Kumar et al. 2000; Sarkar et al. 2025). Moreover, it has been found that all the proteins of SUF system belongs to Fe–S cluster formation. Secondary structure analysis showed that, α helices accounted for an average of 41% of the total secondary structure. The predominance of α helices suggested that these proteins had stable core structure which is essential for maintaining it integrity under stress condition, and also crucial for providing stability and backbone through hydrogen bonding. The proportion of beta turn for all the SUF proteins is ~ 5.77%. Although β turn occupied a small portion, they are essential for compact folding and proper spatial arrangement of protein. They may connect different structural elements (e.g., α helices and β sheets) and contribute to the formation of active sites or ligand-binding pockets. The combined presence of β sheets and extended strands (~ 37.02%), suggests a robust structural framework. This rigidity is crucial for proteins like SufB and SufD, which form the core of scaffold complex and provide a stable platform for Fe–S cluster assembly. The substantial presence of coils indicates that the protein has flexible regions, allowing it to adapt to conformational changes during Fe–S cluster assembly and transfer (Choby et al. 2016; Blahut et al. 2020; Dussouchaud et al. 2024).

Model selection and validation

All models had GMQE value > 0.8 with sequence identity of more than 90%. MolProbity confirmed that > 90% residues were situated within the favored region. Additionally, selected models passed backbone geometry and torsion angle with significant scores. Evaluation of ERRAT scores (> 80%) across models indicated that models were of high quality. All the selected models have a GMQE value > 0.8 and sequence identity is > 90%. (Figs. S2 to S4, and Table S3).

Compound selection for targeting SUF proteins and molecular docking

SUF system plays a crucial role in Fe–S cluster assembly, particularly under oxidative stress and Fe limiting conditions and is indispensable for bacterial survival when ISC system is compromised. Unlike human cells, which primarily rely on the mitochondrial ISC (Fe–S Cluster) pathway, many pathogenic bacteria (*Staphylococcus hominis*, *Microbacterium tuberculosis*) depend predominantly on the SUF system (Garcia et al. 2019). Previous studies have reported SUF inhibitors in pathogens such as *Mycobacterium tuberculosis*, *Enterococcus faecalis*, and *Plasmodium falciparum* (Blahut et al. 2020). Additionally, compounds such as 882 and D-cycloserine have shown inhibitory effects on Fe–S cluster biogenesis (Huet et al. 2005; Charan et al. 2014). Considering the rise of antibiotic resistance, structure-based virtual screening was performed to identify potential inhibitors against eight SUF-associated proteins (SufB, SufC, SufD, PaaD, ApbC, IscR, cysteine desulfurase, and SufE2).

Within the genome of BRTN, presence of SufB, SufC, and SufD is a clear indication of presence of a functional SUF system. Previous study reported that 882 compound (PubChem CID 719865) inhibited aconitase activity by targeting SufC (Choby et al. 2016). However, our docking analysis (Figs. S10 to S37, and Tables S4 and S5) revealed that, 882 exhibited the strongest binding affinity with Apbc (Vina score − 9.1) followed by SufD and IScR (Vina score − 8.2). Its affinity for SufC was comparatively lower (− 7.2). The higher affinity toward ApbC was primarily driven by polar contacts, suggesting a more statically stable complex, possibly impeding cofactor exchange or substrate turnover. In contrast, binding to SufC involved π–π and π–σ interactions, which are often associated with non-covalent anchoring in hydrophobic pockets. Given that SufC functions as an ATPase, such interactions may hinder necessary domain motions required for ATP hydrolysis and Fe–S cluster assembly (Williams et al. 2004). The interaction with sufD likely affects the SufBCD complex assembly, whereas IscR binding, enriched with π–alkyl and π–cation contacts, may interfere with DNA-binding or redox-sensing capacity (Rajagopalan et al. 2013). Hydrogen bonds, particularly N–H···O types, play critical role in orienting ligands within the binding pockets, while π–π stacking interactions significantly enhance binding affinity (Ferreira de Freitas and Schapira 2017; Gallina et al. 2014). Consistent with this, our docking results indicated that most SUF proteins exhibited strong binding affinities with ligands forming multiple hydrogen bonds complemented by hydrophobic and aromatic interactions. Among all proteins, SufD showed the highest binding affinity with ChEMBL3962891 (Vina score − 14.4; Fig. 7), followed by ChEMBL3912062 (− 9.5), driven by hydrogen bonding and extensive hydrophobic contacts, suggesting strong conformational stabilization of the binding pocket. SufC showed highest affinity with CHEMBL3908295 (-8.6), where π–π and π–sulfur interactions were predominant, which indicates possible interference with ATP hydrolysis. Additionally, SufB has the best interaction with two compounds ofloxacin, and ChEMBL3921511 with Vina score of -9.7, and -9.6 respectively. IscR showed highest binding affinity with ChEMBL3908295 (–9.4), suggesting that aromatic and charged residues in its DNA-binding domain contribute to ligand stabilization (Rajagopalan et al. 2013). For SufE2, the top interaction with CHEMBL3718414 suggested the ligand-binding pocket of SufE2 accommodates hydrophobic and charged groups, possibly contributing to its functional flexibility. ApbC and cysteine desulfurase were also notable targets, with compound 882 (positive control) showed strong binding to ApbC (− 9.1), consistent with previous reports on its inhibitory effect on aconitase activity via SUF protein targeting (Choby et al. 2016). Similarly, cysteine desulfurase displayed strong interactions with CHEMBL3908295 and CHEMBL3651495 (− 9.3 and − 9.1). Cycloserine did not exhibit any significant affinity toward SUF proteins in this study due to limited hydrophobic and aromatic features. Unlike fluoroquinolones or other selected ligands, cycloserine lacks extended aromatic scaffolds and halogen substitutions that could enhance π-stacking or halogen bonding, which are critical for high-affinity binding (Lu et al. 2012).

When evaluating binding affinities of antibiotics across generations, third and fourth-generation antibiotics demonstrated higher docking scores with SUF proteins, implying better binding potential. Notably, SufB showed the highest affinity with Ofloxacin, a second-generation fluoroquinolone, suggesting the potential broad-spectrum binding versatility of this protein. Structural modifications introduced in later-generation fluoroquinolones, including additional halogen substitutions and extended aromatic moieties, likely enhanced π–π stacking, hydrophobic interactions, and halogen bonding (Gallina et al. 2014). The interaction profile of Ofloxacin with SufB was dominated by a conventional

Fig. 7 Docking of SufD with top 9 compounds showing Vina scores and their PubChem IDs

hydrogen bond (Met), carbon–hydrogen bond (Thr), and π–alkyl and π–π stacked interactions (Pro, Trp), consistent with previous findings that hydrophobic and aromatic interactions are key determinants of high-affinity ligand binding (Ferreira de Freitas and Schapira 2017). Overall, conventional hydrogen bonds emerged as the dominant interaction type, followed by π–alkyl and carbon-hydrogen contacts, in agreement with earlier findings that efficient ligands often rely on hydrophobic stabilization rather than excessive hydrogen bonding (Ferreira de Freitas and Schapira 2017; Kuhn et al. 2020). These results suggested that SUF proteins, particularly SufD, SufC, and ApbC represented promising drug targets, and several identified ligands showed comparable or superior binding potential to the known inhibitor 882.

In summary, mud volcano sample has been collected and characterized its elemental composition, and observed a notably high iron concentration. Upon culturing the sample, ten distinct bacterial colonies were found, among which BRTN exhibited the highest iron tolerance (up to 600 mg

L^{-1}). To investigate potential co-selection or cross-resistance mechanisms, antibiotic resistance patterns had been analyzed, as a result BRTN displayed resistance to aminoglycosides antibiotics as per CLSI (2020). Interestingly, both high iron exposure and aminoglycoside treatment exert oxidative stress on bacteria, however, BRTN demonstrated resilience under both metal and antibiotics treatments. To unveil the molecular basis for this oxidative stress resistance, whole-genome sequencing was conducted and identified the presence of SUF system, responsible for mitigating oxidative stress. Furthermore, structural validation of SUF components supported its functionality. Unlike pathogenic bacteria that utilize oxidative stress systems for virulence, SUF appeared to be a core defense mechanism in BRTN also. Given its absence in humans, it might be proposed that SufD could be a potential inhibitor against bacterial pathogenicity.

Conclusion

The present experimental analysis showed potentiality of a bacterial isolate from mud volcano sources. As the mud volcanoes represent polyextreme ecosystem, the resident bacterial strains may exhibit unique features with possible applications in biotechnology, environmental remediation, and antimicrobial therapy. Whole genome sequencing and molecular analysis identified BRTN as *Bacillus* sp. Whereas, in silico analysis detected the presence of SUF proteins as essential in nature and non-homologous to *Homo sapiens*. Moreover, BRTN did not show extreme pathogenicity confirmed by VFDB and CARD tool. Protein ligand interaction targeting SUF system predicted through computational analysis found that SufD could be a potent drug target showing highest vina score (ligand ChEMBL3921511 = − 14.4), which was higher than already reported inhibitor compound 882 (PubChem CID 719865). Notably, compound 882 and ChEMBL3962891 exhibited conventional hydrogen (882-2, Ser, Arg; ChEMBL3962891-Arg) bonding, and π-alkyl (3-Ile, Ile, Arg; ChEMBL3962891-Val) bond. Therefore, we suggest inhibitor compounds like ChEMBL3962891 may be applicable as potential drug against bacteria. These findings not only contribute to the search for novel antimicrobials but also support global efforts in combating AMR, aligned with the United Nations Sustainable Development Goals (SDG 3: Good Health and Well-being, and SDG 9: Industry, Innovation, and Infrastructure), fostering the development of new therapeutic strategies to address the growing global health crisis aligning with the concept of "one health".

Supplementary Information The online version contains supplementary material available at https://doi.org/10.1007/s00203-025-04480-3.

Acknowledgements KS, DK, AK, ML, RB are thankful to the UGC Centre for Advanced Study, Department of Botany, The University of Burdwan and DST-FIST, for pursuing research activities and facilities. Karuna Soren is thankful to CSIR for providing a Junior Research Fellowship [File no. 09/0025(17083)/2023-EMR-I; CSIR-JRF June, 2022] during this research work. AK is thankful to WB-DST [Memo No. 819(Sanc.)/STBT-11012(11)/11/2020-STSEC]. DK [File no. 211610042266] and ML [UGC Ref. No.: 737] are thankful to UGC for providing Junior Research Fellowship and Senior Research Fellowship, respectively during this research work. Authors are thankful to University Science Instrumentation Centre (USIC), The University of Burdwan. Central Instrumentation Facility (CIF), BIT Meshra, Ranchi, Jharkhand, and ICRISAT for elemental analyses and genome sequencing, respectively. Mr. Rajdeep Shaw of The University of Burdwan helped in generation of QGIS map.

Author contribution KS conducted the experiments, analysed all data, wrote the original draft, and conceptualization of the work. DK conducted the in silico work, and analysis. AK performed the figure correction, formal analysis of the data, and reviewed the original draft. UH conducted some of experimental part (genomic analyses). ML reviewed and wrote a part of manuscript. AC, and RKV performed the whole genome sequencing. AB, and RB collected the mud sample, and edited the original draft. RB conceptualised, supervised the research work, and edited the manuscript thoroughly.

Funding No funding has been received for this study.

Availability of data and materials The datasets generated during and/or analysed during the current study are available from the corresponding author on reasonable request.

Declarations

Conflict of interest All the authors declare they have no conflict of interest.

Informed consent Not applicable.

References

Alnaimat S, Shattal S, Althunibat O et al (2017) Iron (II) and other heavy-metal tolerance in bacteria isolated from rock varnish in the arid region of Al-Jafer Basin, Jordan. Biodiversitas 18:1250–1257. https://doi.org/10.13057/biodiv/d180350

Andrews S (2010) FastQC: a quality control tool for high throughput sequence data. Babraham Bioinformatics

Andrews SC, Robinson AK, Rodríguez-Quiñones F (2003) Bacterial iron homeostasis. FEMS Microbiol Rev 27:215–237. https://doi.org/10.1016/S0168-6445(03)00055-X

Aqel H, Farah H, Al-Hunaiti A (2024) Ecological versatility and biotechnological promise: comprehensive characterization of the isolated thermophilic Bacillus strains. PLoS One 19:e0297217. https://doi.org/10.1371/journal.pone.0297217

Aziz RK, Bartels D, Best AA et al (2008) The RAST server: rapid annotations using subsystems technology. BMC Genom 9:1–15. https://doi.org/10.1186/1471-2164-9-75

Banerjee S, Nandy SK, Chakraborti S (2019) Oxidative Stress as a Determinant of Antimicrobial Action, Resistance, and Treatment. In oxidative stress in microbial diseases. Springer, Singapore, pp 111–124. https://doi.org/10.1007/978-981-13-8763-0_7

Bankevich A, Nurk S, Antipov D et al (2012) SPAdes: a new genome assembly algorithm and its applications to single-cell sequencing. J Comput Biol 19:455–477. https://doi.org/10.1089/cmb.2012.0021

Baran A, Kwiatkowska A, Potocki L (2023) Antibiotics and bacterial resistance—a short story of an endless arms race. Int J Mol Sci 24:5777. https://doi.org/10.3390/ijms24065777

Bauer AW, Kirby WMM, Sherris JC, Turck M (1966) Antibiotic susceptibility testing by a standardized single disk method. Am J Clin Pathol 45:493–496. https://doi.org/10.1093/ajcp/45.4_ts.493

Benítez-Mateos AI, Paradisi F (2023) *Halomonas elongata*: a microbial source of highly stable enzymes for applied biotechnology. Appl Microbiol Biotechnol 107:3183–3190. https://doi.org/10.1007/s00253-023-12510-7

Blahut M, Sanchez E, Fisher CE, Outten FW (2020) Fe-S cluster biogenesis by the bacterial Suf pathway. Biochimica Et Biophys Acta (BBA) Mol Cell Res. https://doi.org/10.1016/j.bbamcr.2020.118829

Bolger AM, Lohse M, Usadel B (2014) Trimmomatic: a flexible trimmer for Illumina sequence data. Bioinformatics 30:2114–2120. https://doi.org/10.1093/bioinformatics/btu170

Charan M, Singh N, Kumar B et al (2014) Sulfur mobilization for fe-s cluster assembly by the essential suf pathway in the *Plasmodium falciparum* apicoplast and its inhibition. Antimicrob Agents Chemother 58:3389–3398. https://doi.org/10.1128/AAC.02711-13

Chen S-C, Chen M-F, Lai M-C et al (2015) *Methanoculleus sediminis* sp. nov., a methanogen from sediments near a submarine mud volcano. Int J Syst Evol Microbiol 65:2141–2147. https://doi.org/10.1099/ijs.0.000233

Choby JE, Mike LA, Mashruwala AA(2016) A small-molecule inhibitor of iron-sulfur cluster assembly uncovers a link between virulence regulation and metabolism in *Staphylococcus aureus*. Cell Chem Biol 23:1351–1361. https://doi.org/10.1016/j.chembiol.2016.09.012

Colclough AL, Scadden J, Blair JMA (2019) TetR-family transcription factors in Gram-negative bacteria: conservation, variation and implications for efflux-mediated antimicrobial resistance. BMC Genom 20:1–12. https://doi.org/10.1186/s12864-019-6075-5

Cornelis P, Wei Q, Andrews SC, Vinckx T (2011) Iron homeostasis and management of oxidative stress response in bacteria. Metallomics 3:540–549. https://doi.org/10.1039/c1mt00022e

Da Cunha V, Guérillot R, Brochet M, Glaser P (2022) Integrative and conjugative elements encoding DDE transposases. In: Roberts AP, Mullany P (eds) Bacterial integrative mobile genetic elements. CRC Press, pp 250–260. https://doi.org/10.1201/9780367813925

Daou N, Buisson C, Gohar M, Vidic J, Bierne H, Kallassy M, Lereclus D, Nielsen-LeRoux C (2009) IlsA, a unique surface protein of Bacillus cereus required for iron acquisition from heme, hemoglobin and ferritin. PLoS Pathog 5:e1000675. https://doi.org/10.1371/journal.ppat.1000675

Darling ACE, Mau B, Blattner FR, Perna NT (2004) Mauve: multiple alignment of conserved genomic sequence with rearrangements. Genome Res 14:1394–1403. https://doi.org/10.1101/gr.2289704

Davies J (1990) What are antibiotics? Archaic functions for modern activities. Mol Microbiol 4:1227–1232. https://doi.org/10.1111/j.1365-2958.1990.tb00701.x

Dhaker AS, Marwah R, Damodar R et al (2011) In vitro evaluation of antioxidant and radioprotective properties of a novel extremophile from mud volcano: implications for management of radiation emergencies. Mol Cell Biochem 353:243–250. https://doi.org/10.1007/s11010-011-0792-7

Dimitrov LI (2002) Mud volcanoes—the most important pathway for degassing deeply buried sediments. Earth Sci Rev 59:49–76. https://doi.org/10.1016/S0012-8252(02)00069-7

Dowling A, O'Dwyer J, Adley C (2017) Antibiotics: mode of action and mechanisms of resistance. Antimicrob Res Nov Bioknowl Educ Programs 1:536–545

Dussouchaud M, Barras F, de Choudens SO (2024) Fe-S biogenesis by SMS and SUF pathways: a focus on the assembly step. Biochim Et Biophys Acta (BBA) Mol Cell Res 1871:119772. https://doi.org/10.1016/j.bbamcr.2024.119772

Elchennawi I, Ollagnier de Choudens S (2022) Iron–sulfur clusters toward stresses: implication for understanding and fighting tuberculosis. Inorganics (Basel) 10:174. https://doi.org/10.3390/inorganics10100174

Esquilin-Lebron K, Dubrac S, Barras F, Boyd JM (2021) Bacterial approaches for assembling iron-sulfur proteins. Mbio 12:e02425–21. https://doi.org/10.1128/mBio.02425-21

Ezraty B, Vergnes A, Banzhaf M et al (2013) Fe-S cluster biosynthesis controls uptake of aminoglycosides in a ROS-less death pathway. Science 340:1583–1587. https://doi.org/10.1126/science.1238328

Ferreira de Freitas R, Schapira M (2017) A systematic analysis of atomic protein–ligand interactions in the PDB. Medchemcomm 8:1970–1981. https://doi.org/10.1039/C7MD00381A

Fokunang ET, Fokunang CN (2022) Overview of the advancement in the drug discovery and contribution in the drug development process. J Adv Med Pharm Sci 24:10–32. https://hal.science/hal-05194760

Fontecave M, Ollagnier-de-Choudens S (2008) Iron–sulfur cluster biosynthesis in bacteria: mechanisms of cluster assembly and transfer. Arch Biochem Biophys 15:226–37. https://doi.org/10.1016/j.abb.2007.12.014

Fru EC, Piccinelli P, Fortin D (2012) Insights into the global microbial community structure associated with iron oxyhydroxide minerals deposited in the aerobic biogeosphere. Geomicrobiol J 29:587–610. https://doi.org/10.1080/01490451.2011.599474

Galera-Laporta L, Comerci CJ, Garcia-Ojalvo J, Süel GM (2021) Ionobiology: the functional dynamics of the intracellular metallome, with lessons from bacteria. Cell Syst 12:497–508. https://doi.org/10.1016/j.cels.2021.04.011

Gallina AM, Bork P, Bordo D (2014) Structural analysis of protein-ligand interactions: the binding of endogenous compounds and of synthetic drugs. J Mol Recognit 27:65–72. https://doi.org/10.1002/jmr.2332

Gao F (2020) Iron–sulfur cluster biogenesis and iron homeostasis in cyanobacteria. Front Microbiol 11:165. https://doi.org/10.3389/fmicb.2020.00165

Garcia PS, Gribaldo S, Py B, Barras F (2019) The SUF system: an ABC ATPase-dependent protein complex with a role in Fe–S cluster biogenesis. Res Microbiol 170:426–434. https://doi.org/10.1016/j.resmic.2019.08.001

Garcia PS, D'angelo F, Ollagnier de Choudens S et al (2022) An early origin of iron–sulfur cluster biosynthesis machineries before Earth oxygenation. Nat Ecol Evol 6:1564–1572. https://doi.org/10.1038/s41559-022-01857-1

Geourjon C, Deleage G (1995) SOPMA: significant improvements in protein secondary structure prediction by consensus prediction from multiple alignments. Bioinformatics 11:681–684. https://doi.org/10.1093/bioinformatics/11.6.681

Gorityala N, Baidya AS, Sagurthi SR (2024) Genome mining of *Mycobacterium tuberculosis*: targeting SufD as a novel drug candidate through in silico characterization and inhibitor screening. Front Microbiol. https://doi.org/10.3389/fmicb.2024.1369645

Grant JR, Enns E, Marinier E et al (2023) Proksee: in-depth characterization and visualization of bacterial genomes. Nucleic Acids Res 51:W484–W492. https://doi.org/10.1093/nar/gkad326

Guillouzo A, Guguen-Guillouzo C (2020) Antibiotics-induced oxidative stress. Curr Opin Toxicol 20:23–28. https://doi.org/10.1016/j.cotox.2020.03.004

Guruprasad K, Reddy BVB, Pandit MW (1990) Correlation between stability of a protein and its dipeptide composition: a novel approach for predicting in vivo stability of a protein from its primary sequence. Protein Eng des Sel 4:155–161. https://doi.org/10.1093/protein/4.2.155

Halder U, Banerjee A, Biswas R et al (2020) Production of prodigiosin by a drug-resistant *Serratia rubidaea* HB01 isolated from sewage. Environ Sustain 3:279–287. https://doi.org/10.1007/s42398-020-00115-z

Halder U, Biswas R, Kabiraj A et al (2022) Genomic, morphological, and biochemical analyses of a multi-metal resistant but multi-drug susceptible strain of *Bordetella petrii* from hospital soil. Sci Rep 12:8439. https://doi.org/10.1038/s41598-022-12435-7

Hannig C, Hannig M, Rehmer O et al (2007) Fluorescence microscopic visualization and quantification of initial bacterial colonization on enamel *in situ*. Arch Oral Biol 52:1048–1056. https://doi.org/10.1016/j.archoralbio.2007.05.006

Harris DP (1993) Mineral resource stocks and information. In: Kneese AV, Sweeney JL (eds) Handbook of natural resource and energy economics. Elsevier, pp 1011–1076. https://doi.org/10.1016/S1573-4439(05)80008-9

Hemkemeyer M, Schwalb SA, Heinze S et al (2021) Functions of elements in soil microorganisms. Microbiol Res 252:126832. https://doi.org/10.1016/j.micres.2021.126832

Holding AJ, Collee JG (1971) Chapter I routine biochemical tests. In: Norris JR, Ribbons DW (eds) Methods in microbiology. Elsevier, pp 1–32. https://doi.org/10.1016/S0580-9517(08)70573-7

Huet G, Daffé M, Saves I (2005) Identification of the *Mycobacterium tuberculosis* SUF machinery as the exclusive mycobacterial system of [Fe-S] cluster assembly: evidence for its implication in the pathogen's survival. J Bacteriol 187:6137–6146. https://doi.org/10.1128/JB.187.17.6137-6146.2005

Ilayaraja S, Rajkumar J, Swarnakumar NS et al (2014) Isolation of two thermophilic actinobacterial strains mud volcano of the Baratang Island, India. Afr J Microbiol Res 8:40–45. https://doi.org/10.5897/AJMR09.126

Jackman SD, Vandervalk BP, Mohamadi H et al (2017) ABySS 2.0: resource-efficient assembly of large genomes using a Bloom filter. Genome Res 27:768–777. https://doi.org/10.1101/gr.214346.116

Jinal HN, Gopi K, Prittesh P et al (2019) Phytoextraction of iron from contaminated soils by inoculation of iron-tolerant plant growth-promoting bacteria in *Brassica juncea* L. Czern Environ Sci Pollut Res 26:32815–32823. https://doi.org/10.1007/s11356-019-06394-2

Jones TS, Oliveira SMD, Myers CJ et al (2022) Genetic circuit design automation with Cello 2.0. Nat Protoc 17:1097–1113. https://doi.org/10.1038/s41596-021-00675-2

Klebba PE, Newton SMC, Six DA et al (2021) Iron acquisition systems of gram-negative bacterial pathogens define TonB-dependent pathways to novel antibiotics. Chem Rev 121:5193–5239. https://doi.org/10.1021/acs.chemrev.0c01005

Kircher M (2011) Analysis of high-throughput ancient DNA sequencing data. InAncient DNA: methods and protocols. Humana Press, Totowa, NJ, pp 197–228. https://doi.org/10.1007/978-1-61779-516-9_23

Kokoschka S, Dreier A, Romoth K et al (2015) Isolation of anaerobic bacteria from terrestrial mud volcanoes (Salse di Nirano, Northern Apennines, Italy). Geomicrobiol J 32:355–364. https://doi.org/10.1080/01490451.2014.940632

Krivoshein PK, Volkov DS, Rogova OB, Proskurnin MA (2022) FTIR photoacoustic and ATR spectroscopies of soils with aggregate size fractionation by dry sieving. ACS Omega 7:2177–2197. https://doi.org/10.1021/acsomega.1c05702

Kuhn M, Firth-Clark S, Tosco P, Mey AS, Mackey M, Michel J (2020) Assessment of binding affinity via alchemical free-energy calculations. J Chem Inf Model 60:3120–3130. https://doi.org/10.1021/acs.jcim.0c00165

Kumar S, Tsai C-J, Nussinov R (2000) Factors enhancing protein thermostability. Protein Eng 13:179–191. https://doi.org/10.1093/protein/13.3.179

Lankford CE, Byers BR (1973) Bacterial assimilation of iron. CRC Crit Rev Microbiol 2:273–331. https://doi.org/10.3109/10408417309108388

Liu Y, Yang X, Gan J et al (2022) CB-dock2: improved protein–ligand blind docking by integrating cavity detection, docking and homologous template fitting. Nucleic Acids Res 50:W159–W164. https://doi.org/10.1093/nar/gkac394

Liu W, Xu Y, Slaveykova VI (2023) Oxidative stress induced by sub-lethal exposure to copper as a mediator in development of bacterial resistance to antibiotics. Sci Total Environ 860:160516. https://doi.org/10.1016/j.scitotenv.2022.160516

Lo Sciuto A, D'Angelo F, Spinnato MC et al (2024) A molecular comparison of [Fe-S] cluster-based homeostasis in Escherichia coli and Pseudomonas aeruginosa. Mbio 15:e01206-e1224. https://doi.org/10.1128/mbio.01206-24

Loiseau L, Ollagnier-de-Choudens S, Nachin L et al (2003) Biogenesis of Fe-S cluster by the bacterial Suf system: SufS and SufE form a new type of cysteine desulfurase. J Biol Chem 278:38352–38359. https://doi.org/10.1074/jbc.M305953200

Lu Y, Liu Y, Xu Z et al (2012) Halogen bonding for rational drug design and new drug discovery. Expert Opin Drug Discov 7:375–383. https://doi.org/10.1517/17460441.2012.678829

Luo H, Lin Y, Liu T et al (2021) DEG 15, an update of the database of essential genes that includes built-in analysis tools. Nucleic Acids Res 49:D677–D686. https://doi.org/10.1093/nar/gkaa917

Manna SK, Das BK, Mohanty BP et al (2021) Exploration of heterotrophic bacterial diversity in sediments of the mud volcano in the Andaman and Nicobar Islands, India. Environ Nanotechnol Monit Manag 16:100465. https://doi.org/10.1016/j.enmm.2021.100465

Mashruwala AA, Bhatt S, Poudel S et al (2016) The DUF59 containing protein SufT is involved in the maturation of iron-sulfur (FeS) proteins during conditions of high FeS cofactor demand in *Staphylococcus aureus*. PLoS Genet 12:e1006233. https://doi.org/10.1371/journal.pgen.1006233

Matkawala F, Nighojkar S, Kumar A, Nighojkar A (2021) Microbial alkaline serine proteases: production, properties and applications. World J Microbiol Biotechnol 37:1–12. https://doi.org/10.1007/s11274-021-03036-z

McArthur AG, Waglechner N, Nizam F et al (2013) The comprehensive antibiotic resistance database. Antimicrob Agents Chemother 57:3348–3357. https://doi.org/10.1128/aac.00419-13

Meena B, Anburajan L, Aryamol K et al (2023) Studies on biodiversity and bioprospecting of active mud volcano associated bacteria and actinobacteria from Baratang, Andaman Islands, India. Syst Microbiol Biomanuf 3:339–357. https://doi.org/10.1007/s43393-022-00118-3

Meier-Kolthoff JP, Göker M (2019) TYGS is an automated high-throughput platform for state-of-the-art genome-based taxonomy. Nat Commun 10:2182. https://doi.org/10.1038/s41467-019-10210-3

Mikheenko A, Saveliev V, Hirsch P, Gurevich A (2023) WebQUAST: online evaluation of genome assemblies. Nucleic Acids Res 51:W601–W606. https://doi.org/10.1093/nar/gkad406

Muzawazi ES, Thusabantu N, Oluwalana-Sanusi AE et al (2024) Surface-loaded Fe2O3-biochar for the abatement of antibiotics from pharmaceutical wastewater. Int J Environ Sci Technol 21:3827–3844. https://doi.org/10.1007/s13762-023-05201-3

Nambi S, Long JE, Mishra BB et al (2015) The oxidative stress network of *Mycobacterium tuberculosis* reveals coordination between

radical detoxification systems. Cell Host Microbe 17:829–837. https://doi.org/10.1016/j.chom.2015.05.008
Nerber HN, Sorg JA (2021) The small acid-soluble proteins of *Clostridioides difficile* are important for UV resistance and serve as a check point for sporulation. PLoS Pathog 17:e1009516. https://doi.org/10.1371/journal.ppat.1009516
Omoregie EO, Mastalerz V, de Lange G et al (2008) Biogeochemistry and community composition of iron-and sulfur-precipitating microbial mats at the Chefren mud volcano (Nile Deep Sea Fan, Eastern Mediterranean). Appl Environ Microbiol 74:3198–3215. https://doi.org/10.1128/AEM.01751-07
Ozer EA, Allen JP, Hauser AR (2014) Characterization of the core and accessory genomes of *Pseudomonas aeruginosa* using bioinformatic tools Spine and AGEnt. BMC Genom 15:1–17. https://doi.org/10.1186/1471-2164-15-737
Pal C, Bengtsson-Palme J, Kristiansson E, Larsson DGJ (2015) Co-occurrence of resistance genes to antibiotics, biocides and metals reveals novel insights into their co-selection potential. BMC Genom 16:1–14. https://doi.org/10.1186/s12864-015-2153-5
Pala ZR, Saxena V, Saggu GS et al (2019) Functional analysis of iron-sulfur cluster biogenesis (SUF pathway) from *Plasmodium vivax* clinical isolates. Exp Parasitol 198:53–62. https://doi.org/10.1016/j.exppara.2019.01.015
Pardoux R, Fiévet A, Carreira C et al (2019) The bacterial MrpORP is a novel Mrp/NBP35 protein involved in iron-sulfur biogenesis. Sci Rep 9:712. https://doi.org/10.1038/s41598-018-37021-8
Pasqua M, di Bonaccorsi Patti MC, Fanelli G et al (2021) Host-bacterial pathogen communication: the wily role of the multidrug efflux pumps of the MFS family. Front Mol Biosci 8:723274. https://doi.org/10.3389/fmolb.2021.723274
Pelczer MJ (1957) Manual of microbiological methods. Mc Graw-Hill Co., New York
Pérard J, Ollagnier de Choudens S (2018) Iron–sulfur clusters biogenesis by the SUF machinery: close to the molecular mechanism understanding. J Biol Inorg Chem 23:581–596. https://doi.org/10.1007/s00775-017-1527-3
Peters JE, Makarova KS, Shmakov S, Koonin EV (2017) Recruitment of CRISPR-Cas systems by Tn7-like transposons. Proc Natl Acad Sci USA 114:E7358–E7366. https://doi.org/10.1073/pnas.1709035114
Petukhov M, Kil Y, Kuramitsu S, Lanzov V (1997) Insights into thermal resistance of proteins from the intrinsic stability of their α-helices. Proteins Struct Funct Genet 29:309–320. https://doi.org/10.1002/(SICI)1097-0134(199711)29:3%3C309::AID-PROT5%3E3.0.CO;2-5
Pheepakpraw J, Sinchao C, Sutheeworapong S, Sattayawat P, Panya A, Tragoolpua Y, Chitov T (2025) Cytotoxicity and Genome Characteristics of an Emetic Toxin-Producing Bacillus cereus Group sp. Isolated from Raw Milk. Foods 14:485. https://doi.org/10.3390/foods14030485
Plumlee GS, Casadevall TJ, Wibowo HT et al (2008) Preliminary analytical results for a mud sample collected from the LUSI mud volcano, Sidoarjo, East Java, Indonesia. US Geol Surv Open File Rep 1019:10–3133
Prior RB, Perkins RL (1974) Artifacts induced by preparation for scanning electron microscopy in *Proteus mirabilis* exposed to carbenicillin. Can J Microbiol 20:794–795. https://doi.org/10.1139/m74-122
Pronk JT, Johnson DB (1992) Oxidation and reduction of iron by acidophilic bacteria. Geomicrobiol J 10:153–171. https://doi.org/10.1080/01490459209377918
Py B, Barras F (2010) Building Fe–S proteins: bacterial strategies. Nat Rev Microbiol 8:436–446. https://doi.org/10.1038/nrmicro2356
Rajagopalan S, Teter SJ, Zwart PH et al (2013) Studies of IscR reveal a unique mechanism for metal-dependent regulation of DNA binding specificity. Nat Struct Mol Biol 20:740–747. https://doi.org/10.1038/nsmb.2568
Raphenya AR, Robertson J, Jamin C, de Oliveira Martins L, Maguire F, McArthur AG, Hays JP (2022) Datasets for benchmarking antimicrobial resistance genes in bacterial metagenomic and whole genome sequencing. Scientific data 9:341. https://doi.org/10.1038/s41597-022-01463-7
Ratnikova NM, Slobodkin AI, Merkel AY et al (2020) *Sulfurimonas crateris* sp. nov., a facultative anaerobic sulfur-oxidizing chemolithoautotrophic bacterium isolated from a terrestrial mud volcano. Int J Syst Evol Microbiol 70:487–492. https://doi.org/10.1099/ijsem.0.003779
Rekik H, Jaouadi NZ, Gargouri F et al (2019) Production, purification and biochemical characterization of a novel detergent-stable serine alkaline protease from *Bacillus safensis* strain RH12. Int J Biol Macromol 121:1227–1239. https://doi.org/10.1016/j.ijbiomac.2018.10.139
Rolfe MD, Rice CJ, Lucchini S et al (2012) Lag phase is a distinct growth phase that prepares bacteria for exponential growth and involves transient metal accumulation. J Bacteriol 194:686–701. https://doi.org/10.1128/jb.06112-11
Sarkar S, Yadav M, Kumar A (2025) Analysing microbial proteins: bioinformatic approaches for molecular structure and function characterization. In: Parray JA, Singh N, Li W-J (eds) Computational genomics and structural bioinformatics in microbial science. Elsevier, pp 29–51. https://doi.org/10.1016/B978-0-443-31550-3.00002-0
Seemann T (2014) Prokka: rapid prokaryotic genome annotation. Bioinformatics 30:2068–2069. https://doi.org/10.1093/bioinformatics/btu153
Sholehhudin M, Susanto BH, Adriyani R, Laksono D (2019) Heavy metals contamination in groundwater around Sidoarjo Mud Vulcano Area, East Java Indonesia. Malays J Med Health Sci 15:86–89
Shylla L, Barik SK, Joshi SR (2021) Characterization and bioremediation potential of native heavy-metal tolerant bacteria isolated from rat-hole coal mine environment. Arch Microbiol 203:2379–2392. https://doi.org/10.1007/s00203-021-02218-5
Slobodkina GB, Merkel AY, Novikov AA et al (2020) *Pelomicrobium methylotrophicum* gen. nov., sp. nov. a moderately thermophilic, facultatively anaerobic, lithoautotrophic and methylotrophic bacterium isolated from a terrestrial mud volcano. Extremophiles 24:177–185. https://doi.org/10.1007/s00792-019-01145-0
Stautz J, Hellmich Y, Fuss MF et al (2021) Molecular mechanisms for bacterial potassium homeostasis. J Mol Biol 433:166968. https://doi.org/10.1016/j.jmb.2021.166968
Touati D (2000) Iron and oxidative stress in bacteria. Arch Biochem Biophys 373:1–6. https://doi.org/10.1006/abbi.1999.1518
Tu T-H, Wu L-W, Lin Y-S et al (2017) Microbial community composition and functional capacity in a terrestrial ferruginous, sulfate-depleted mud volcano. Front Microbiol 8:2137. https://doi.org/10.3389/fmicb.2017.02137
Vaishampayan A, Grohmann E (2022) Antimicrobials functioning through ros-mediated mechanisms: current insights. Microorganisms 10:61. https://doi.org/10.3390/microorganisms10010061
Vats P, Kaur UJ, Rishi P (2022) Heavy metal-induced selection and proliferation of antibiotic resistance: a review. J Appl Microbiol 132:4058–4076. https://doi.org/10.1111/jam.15492
Wendel BM, Pi H, Krüger L et al (2022) A central role for magnesium homeostasis during adaptation to osmotic stress. Mbio. https://doi.org/10.1128/mbio.00092-22
Williams DH, Stephens E, O'Brien DP, Zhou M (2004) Understanding noncovalent interactions: ligand binding energy and catalytic efficiency from ligand-induced reductions in motion within receptors and enzymes. Angewandte Chemie Int Edn 43:6596–6616. https://doi.org/10.1002/anie.200300644

Wollers S, Layer G, Garcia-Serres R et al (2010) Iron-sulfur (Fe-S) cluster assembly: the SufBCD complex is a new type of Fe-S scaffold with a flavin redox cofactor. J Biol Chem 285:23331–23341. https://doi.org/10.1074/jbc.M110.127449

Yang H, Lou K, Sun J et al (2012) Prokaryotic diversity of an active mud volcano in the Usu City of Xinjiang, China. J Basic Microbiol 52:79–85. https://doi.org/10.1002/jobm.201100074

Yu NY, Wagner JR, Laird MR et al (2010) PSORTb 3.0: improved protein subcellular localization prediction with refined localization subcategories and predictive capabilities for all prokaryotes. Bioinformatics 26:1608–1615

Yuda E, Tanaka N, Fujishiro T et al (2017) Mapping the key residues of SufB and SufD essential for biosynthesis of iron-sulfur clusters. Sci Rep 7:9387. https://doi.org/10.1038/s41598-017-09846-2

Zerbino DR, Birney E (2008) Velvet: algorithms for de novo short read assembly using de Bruijn graphs. Genome Res 18:821–829. https://doi.org/10.1101/gr.074492.107

Zhang R, Ou H, Zhang C (2004) DEG: a database of essential genes. Nucleic Acids Res 32:D271–D272. https://doi.org/10.1093/nar/gkh024